

**ENCLOSURE 4**

**MFN-07-445 Supplement 1**

**C. L. Martin, Nuclear Basis for ECCS (Appendix K)  
Calculations, NEDO-23729, Class 1 GE Report, November  
1977**

**Non-Proprietary Version**

NEDO-23729  
77NED306  
CLASS I  
NOVEMBER 1977

DOCUMENT LIBRARY

MAR 6 1978

GENERAL ELECTRIC CO.  
Nuclear Energy Division

**NUCLEAR BASIS FOR  
ECCS (APPENDIX K)  
CALCULATIONS**

**NON-CIRCULATING**

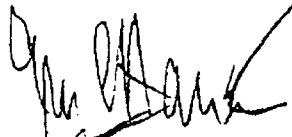
C. L. MARTIN

GENERAL  ELECTRIC

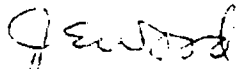
**NUCLEAR BASIS FOR  
ECCS (APPENDIX K) CALCULATIONS**

**C. L. MARTIN**

Approved:

  
E. C. Hansen, Manager  
System Design Automation

Approved:

  
W. E. Wood, Manager  
Nuclear Core Technology

---

NUCLEAR ENERGY ENGINEERING DIVISION • GENERAL ELECTRIC COMPANY  
SAN JOSE, CALIFORNIA 95125

**GENERAL  ELECTRIC**

## DISCLAIMER OF RESPONSIBILITY

*This document was prepared by or for the General Electric Company. Neither the General Electric Company nor any of the contributors to this document:*

- A. Makes any warranty or representation, express or implied, with respect to the accuracy, completeness, or usefulness of the information contained in this document, or that the use of any information disclosed in this document may not infringe privately owned rights; or*
- B. Assumes any responsibility for liability or damage of any kind which may result from the use of any information disclosed in this document.*

**TABLE OF CONTENTS**

	Page
<b>ABSTRACT</b> .....	ix
<b>1. INTRODUCTION</b> .....	1-1
<b>2. BASIC NUCLEAR DATA</b> .....	2-1
2.1 Energy Release per Fission.....	2-1
2.2 Decay Parameters of the Actinides .....	2-16
<b>3. NUCLEAR ENERGY SOURCES</b> .....	3-1
3.1 Evaluation of Energy Sources .....	3-1
3.1.1 Decay Heat from Fission Products.....	3-1
3.1.2 Decay Heat from Actinides.....	3-1
3.1.3 Delayed Neutron Induced Fission Heat.....	3-11
3.1.4 Decay Heat from Structural Materials.....	3-11
3.2 Specifications for Decay Heat Models.....	3-14
<b>4. NUCLEAR ENERGY TRANSPORT AND DEPOSITION</b> .....	4-1
4.1 Evaluation of Energy Transport Models .....	4-1
4.1.1 Gamma and Neutron Energy Deposition.....	4-1
4.1.2 Rod-to-Rod Gamma Energy Transport.....	4-2
4.1.3 Bundle-to-Bundle Gamma Energy Transport.....	4-10
4.2 Specifications for Energy Transport Models.....	4-12
<b>5. NUCLEAR CORE DESIGN DATA</b> .....	5-1
<b>6. CONCLUSIONS</b> .....	6-1
<b>7. REFERENCES</b> .....	7-1

LIST OF ILLUSTRATIONS

Figure	Title	Page
4-1	Rod-by-Rod Gamma Energy Deposition for 8D250 under LOCA Conditions .....	4-5
4-2	Rod-by-Rod Gamma Energy Deposition for BF1T2 under LOCA Conditions .....	4-7
4-3	Rod-by-Rod Gamma Energy Deposition for 8D250 under Normal Power Conditions .....	4-8
4-4	Rod-by-Rod Gamma Energy Deposition for BF1T2 under Normal Power Conditions .....	4-9

LIST OF TABLES

Table	Page
2-1 Energy Release Per Fission of $U^{235}$ .....	2-2
2-2 Energy Release Per Fission of $U^{238}$ .....	2-4
2-3 Energy Release Per Fission of $Pu^{239}$ .....	2-5
2-4 Energy Release Per Fission of $Pu^{241}$ .....	2-6
2-5 Energy Release Per Fission of $U^{233}$ .....	2-7
2-6 Energy Release Per Fission of $Th^{232}$ .....	2-8
2-7 Energy Release Per Fission of $U^{234}$ .....	2-9
2-8 Energy Release Per Fission of $U^{234}$ .....	2-10
2-9 Energy Release Per Fission of $Pu^{240}$ .....	2-11
2-10 Energy Release Per Fission of $Pu^{242}$ .....	2-12
2-11 Summary of Current and Recommended Values for Energy Release Per Fission.....	2-13
2-12 Fractional Energy Release Per Fission in Form of Gamma Rays.....	2-13
2-13 Energy Release Per Capture in Selected Isotopes.....	2-14
2-14 Neutron Capture Rates and Average Energy Release Per Capture for Typical Fuel Designs.....	2-15
2-15 Beta Decay Properties of $U^{239}$ .....	2-16
2-16 Beta Decay Properties of $Np^{239}$ .....	2-17
2-17 Comparison of Old and New Values for the Sensible Beta Decay Energies of $U^{239}$ and $Np^{239}$ .....	2-17
3-1 Tabular Data for the ANS-5 (October 1973) Standard Decay Heat Power for Infinite Reactor Operating Time.....	3-2
3-2 Proposed (ANS-5.1) Tabular Data for Standard Decay Heat Power for Thermal Fission of $U^{235}$ and for Irradiation of $1 \times 10^{13}$ Sec.....	3-3
3-3 Proposed (ANS-5.1) Tabular Data for Standard Decay Heat Power for Fast Fission of $U^{235}$ and for Irradiation of $10^{13}$ Sec.....	3-5
3-4 Proposed (ANS-5.1) Tabular Data for Standard Decay Heat Power for Thermal Fission of $Pu^{239}$ and for Irradiation of $10^{13}$ Sec.....	3-7
3-5 Relative Fission Rate After LOCA.....	3-13
3-6 Properties of Zirconium Isotopes.....	3-13

LIST OF TABLES (Continued)

Table	Title	Page
3-7	Decay Heat Comparison for Different Bundles at Various Exposures and Voids E(GWd/t) .....	3-16
3-8	Decay Heat at T=100 Sec for Bundle 8D250 — Comparison Between Exact Constants and Use of Fits .....	3-20
4-1	Description of Bundles Used in Gamma Transport Calculations .....	4-3
4-2	Gamma Energy Deposition for 8D250 .....	4-3
4-3	Gamma Energy Deposition for 8F1T2 .....	4-4
4-4	Neutron Energy Deposition in Coolant .....	4-4
4-5	Constants for the Rod Power Model .....	4-11
4-6	Constants for the Bundle-to-Bundle Model .....	4-11
4-7	Time Dependence of the Parameters .....	4-14
4-8	Values for Gamma Transport Coefficients .....	4-15
5-1	Values for Gamma Transport Parameter A .....	5-1

**ABSTRACT**

*A comprehensive review of the nuclear basis for ECCS (Appendix K) calculations is presented. The areas covered include: basic nuclear data, nuclear energy sources, nuclear energy transport, and nuclear core design data. New values are proposed for the energy yield per fission of a number of isotopes including U<sup>235</sup>, U<sup>238</sup>, and Pu<sup>239</sup>. A new, more rigorous decay heat model based on the current American Nuclear Society Standard ANS-5 is developed. In addition, a decay heat model based on the ANS-5.1 subcommittee's new decay heat curves is presented for use in evaluating the impact of the proposed standard. In the area of nuclear energy transport, Monte Carlo calculations have been performed to provide more accurate parameters for gamma energy transport.*

## 1. INTRODUCTION

A comprehensive review has been conducted of the nuclear basis for emergency core cooling system (ECCS) calculations, which are required by 10CFR50 Appendix K.<sup>1</sup> The review has been divided into four major areas. The first area covers basic nuclear data including the energy yield per fission of the important fissionable isotopes and the decay parameters and decay energies of the actinides. The second area is concerned with the nuclear sources of heat during a loss-of-coolant accident (LOCA). These sources include decay heat from fission products, decay heat from heavy element actinides, fission heat caused by delayed neutrons, and decay heat from structural materials. The third area of this review is concerned with the way in which the nuclear energy is distributed or deposited in the core. In particular, gamma ray transport effects are evaluated and quantified. The fourth area of this review covers the inputs to ECCS calculations which come directly from nuclear core design calculations. These data include the rod-by-rod fission density and exposure distributions, etc.

Section 2 is concerned solely with basic nuclear data. New values are derived for the energy yield per fission of the isotopes  $U^{235}$ ,  $U^{238}$ , and  $Pu^{239}$ , which are the most significant isotopes for ECCS calculations. In addition, new energy yields are derived for the following isotopes:  $Pu^{241}$ ,  $U^{233}$ ,  $Th^{232}$ ,  $U^{234}$ ,  $U^{236}$ ,  $Pu^{240}$ , and  $Pu^{242}$ . Also included in Section 2 is a discussion of the decay parameters of the actinides  $U^{239}$  and  $Np^{239}$ , which are important to ECCS calculations.

Section 3 covers the area of nuclear energy sources. The four primary sources of energy which were mentioned above, are each given careful consideration. With respect to decay heat from fission products, two sets of data are given. The first set is the current ANS-5 standard<sup>2,3</sup>. The other set is the standard which has been recently proposed by the ANS-5.1 subcommittee on decay heat<sup>4</sup>. Specifications for the combination of the various energy sources into complete decay heat models are given in Subsection 3.2. Three distinct models are presented. The first is identical with the model currently in use. The second is a more rigorous and more accurate model which is still based on the current ANS-5 standard. Finally, the third model is based on the proposed new standard. The latter may not be used in routine calculations since the standard has not yet been approved, but it may be used to evaluate the impact of the proposed standards.

Section 4 is concerned with the ways in which nuclear energy is transported from its source to another region where it is deposited. The primary method for this redistribution of energy is through gamma transport. A secondary method, which is applicable only to normal power conditions, is through neutron energy transport to coolant regions. The results of photon Monte Carlo calculations are presented. These results quantify the amount of gamma energy which is deposited in the various structural components of a fuel bundle and also quantify the redistribution of gamma energy among the fuel rods. Results, previously reported by others<sup>5</sup>, are presented which quantify the effects of gamma transport from one fuel bundle to the next. In Subsection 4.2, specifications are given for including gamma transport effects in ECCS calculations. In addition, a brief review is made of the gamma transport corrections which are currently in use in the process computer.

Section 5 is a brief review of nuclear core design data which have a direct effect on ECCS calculations. Most of these data either have been reviewed elsewhere or are known to have only a small impact in the ECCS area.

Finally, in Section 6, the conclusions of this review of the nuclear basis for ECCS calculations are presented.

## 2. BASIC NUCLEAR DATA

The energy release per fission and the decay parameters of the actinides are of such a fundamental nature that they have been isolated here in a separate section. The principal application of the energy release per fission data to ECCS analyses occurs in the normalization of the decay heat curves. Decay heat data are normally given in terms of power (energy per unit time) divided by fission rate. Dividing this data by the energy release per fission converts the curves into relative power versus time. The actinide decay parameters impact ECCS calculations as one of several components of decay heat. Particular attention must be given to the average energy of the beta decay particles of the actinides, since this determines the *sensible* energy release per decay.

In subsection 2.1, the best available data on the energy release per fission is given for a number of isotopes. Those which are most important for ECCS analyses are  $U^{235}$ ,  $U^{238}$ , and  $Pu^{239}$ . Subsection 2.2 presents the necessary calculations for the decay parameters of the two most significant actinides,  $U^{233}$  and  $Np^{239}$ .

### 2.1 ENERGY RELEASE PER FISSION

There are two general approaches to the problem of determining energy release per fission. The first approach, which is termed the summation method, is to add up all of the separate components of the energy, which may be determined by various experiments. The components consist of the kinetic energy of the fission fragments, the beta and gamma energy released by the decay of fission products, the prompt gamma energy released simultaneously with fission, and the energy of the neutrons which are given off. A subtraction is made of the incident neutron energy, to avoid double counting of this component. The total of all of these components is the sensible energy released *directly* as a consequence of fission. In addition, there is a substantial indirect energy release as a result of the parasitic capture of neutrons in the reactor. The magnitude of this component is different for reactors in separate classes, i.e., BWR, PWR, LMFBR, etc. For reactors within a class, i.e., all BWR's, it is possible to assign a single value. The total energy released in fission is a sum of these direct and indirect sources.

The alternate approach to determining the energy release per fission is the mass excess approach. In this method, data are collected on the yields from fission and the isotopic masses of hundreds of fission products. The difference between the mass of the fissioning isotope and the sum of the yields times the masses of the fission products is the mass excess. In order to compute the sensible energy release it is necessary to subtract from the mass excess the energy which is carried away by antineutrinos and to add on the indirect contribution from capture gammas.

The energy release per fission of  $U^{235}$  is presented in detail in Table 2-1. Five separate calculations from three distinct sources are shown. Since both the summation and mass excess methods are represented, there are unfilled locations in the table whenever a given component does not apply to a particular method. In cases where calculations have been made of components which are not used by a particular method but are nevertheless useful for comparative purposes, the values are enclosed in brackets [ ]. The first column of Table 2-1 presents the summation results of Crowther. These values are currently in use at the General Electric Company for all nuclear design calculations. It is proposed that these values be replaced for several reasons. First of all, the calculations are 8 years old and much new data are available now. Secondly, Crowther neglected to subtract the incident neutron energy. This, of course, is only important for those isotopes which undergo predominantly fast fission such as  $U^{238}$ . A third reason for revising the current values is that the contribution due to capture gammas was computed by obtaining a typical value for the total capture gamma energy release per fission and adding this value to the energy release for each isotope. However, this value is clearly exposure dependent. A more justifiable method was employed by Unik and Gindler<sup>6</sup> and is used in this work. The method consists of computing the average capture gamma energy per fission neutron produced and multiplying this by the number of captured neutrons ( $\nu_i - 1$ ) where  $\nu_i$  is the number of neutrons produced in fission by isotope  $i$ . This results in a different value for the captive gamma energy produced by different isotopes. Further justification of this method will be presented later in this subsection. A final reason for revising the current energy release values is that they include a small correction for fast fissions in the isotopes  $U^{236}$ ,  $Pu^{240}$ ,  $Pu^{242}$ ,  $Np^{237}$ ,  $Am^{243}$ ,  $Cm^{244}$ ,  $Am^{241}$ ,  $Pu^{238}$ ,  $Am^{242}$ , and  $Cm^{242}$ . These fissions were originally ignored in the nuclear design calculations. However, the majority of these fissions occur in the three isotopes  $U^{235}$ ,  $Pu^{240}$  and  $Pu^{242}$  which are now accounted for. Therefore the correction should no longer be applied.

Table 2-1  
**ENERGY RELEASE PER FISSION OF U<sup>235</sup>**  
 (All entries in units of MeV/fission)

Source:	R. L. Crowther (Aug. 1969)	Unik & Gindler (Apr. 1971)		Sher (Oct. 1976)	
		Mass Excess	Summation	LSQ	Systematics
Kinetic Energy of Fragments	169.1		167.9±2.0	[169.58±0.68]	169.1±1.5
Mass Excess		202.74±0.21		202.7±0.1	
Average Beta Energy, $\bar{E}_\beta$	6.71		7.4±0.4	[6.43±0.05]	6.5±0.3
Minus Antineutrinos, $-\bar{E}_\nu$		-10.3±0.6		-8.68±0.06	
Prompt Gamma Energy, $\bar{E}_{\gamma p}$	7.54		7.64±0.75	[6.96±0.70]	7.1±2.0
Delayed Gamma Energy, $\bar{E}_{\gamma d}$	7.63		7.1±1.3	[6.26±0.05]	6.35±0.3
Neutrons:					
Number released, $\nu$	2.434	2.423±0.007	2.423±0.007	2.4188 <sup>a</sup>	
Average Energy, $\bar{E}_n$	1.93				
Total Energy, $\nu\bar{E}_n$	4.71		4.69±0.11		4.79±0.07
Minus Incident Energy, $-\bar{E}_i$	0.0		0.0		0.0
<b>Subtotal</b>	<b>195.69</b>	<b>192.4±0.6</b>	<b>194.73</b>	<b>194.02±0.12</b>	<b>193.8±1.1</b>
Capture Gammas:					
Average Energy, $\bar{E}_{\gamma c}$	5.85 <sup>b</sup>	6.53±.2 <sup>c</sup>	6.53±0.2 <sup>c</sup>	5.46±0.19 <sup>d</sup>	5.46±.019 <sup>d</sup>
Total Energy, $(\nu-1)\bar{E}_{\gamma c}$	8.58	9.29±0.3	9.29±0.3	7.75±0.27	7.75±0.27
Miscellaneous Corrections:	0.17				
<b>Total, Q</b>	<b>204.4</b>	<b>201.7±0.7</b>	<b>204.0</b>	<b>201.8±0.3</b>	<b>201.6</b>

<sup>a</sup>ENDF-B-IV value supplied by C. L. Martin

<sup>b</sup>Computed for TVA fuel design by dividing 8.58 by  $(\nu-1)=1.468$

<sup>c</sup>Computed for EBR-II by Unik and Gindler

<sup>d</sup>Average of three BWR fuel designs at several exposure points

Unik and Gindler<sup>c</sup> performed an extensive review of energy per fission in 1971. They utilized both the mass excess and summation techniques. Their results are presented in the second and third columns of Table 2-1. Note that the error bounds in the mass excess results are much smaller than the bounds in the summation results. The average capture gamma energy of 6.53 MeV reported by Unik and Gindler was computed for EBR-II, an LMFBR. This value is substantially higher than the value of 5.46 MeV which is recommended for a BWR. This is primarily due to the large amount of stainless steel in the EBR-II fuel. Nevertheless, Unik and Gindler's results are presented here because they are well known and are even used in the draft of the new decay heat standard<sup>d</sup>. They are explicitly not recommended, however, for use in nuclear design or ECCS calculations for BWR's.

A very recent evaluation of energy per fission was performed by Sher in 1976<sup>d</sup>. The fourth column in Table 2-1 contains Sher's least squares (LSQ) results, which rely principally on the mass excess calculations of Walker<sup>a</sup> using ENDF-B-IV data. In addition, the LSQ results contain estimates of the other components of the energy release (enclosed in brackets) which were obtained by applying the least squares technique to experimental data, while at the same time maintaining consistency with the mass excess calculations. This is important since a knowledge of the gamma and beta energy components is necessary for decay heat and gamma energy transport calculations. The fifth column of Table 2-1 contains Sher's "Systematics" calculations. These results utilize simplified fits based primarily on the mass and charge, etc., of the fissioning nucleus. These results are most useful for nuclides for which experimental data are unavailable. They are listed in Table 2-1 only to provide a means of assessing the accuracy of the "Systematics" method for other nuclides.

Table 2-2 presents the energy release per fission data for U<sup>238</sup> and Table 2-3 presents the data for Pu<sup>239</sup>. These nuclides along with U<sup>235</sup> are the only important nuclides for ECCS analysis. For completeness, however, energy release per fission data are given for a number of other nuclides in Tables 2-4 through 2-10. These nuclides are Pu<sup>241</sup>, U<sup>233</sup>, Th<sup>232</sup>, U<sup>234</sup>, U<sup>236</sup>, Pu<sup>240</sup>, and Pu<sup>242</sup>. In many cases data are not available from all three sources, but whatever is available is listed in these tables.

The recommended values for energy release per fission for all 10 nuclides are summarized in Table 2-11 alongside the values which are currently used in design. The recommended values for U<sup>235</sup>, U<sup>238</sup>, Pu<sup>239</sup>, Pu<sup>241</sup>, U<sup>233</sup>, and Th<sup>232</sup> are Sher's LSQ results for the direct energy release plus a capture gamma contribution which is appropriate for BWR's. Sher's results were chosen because they are the most recent and evidently the most accurate to date. For the nuclides U<sup>234</sup>, U<sup>236</sup>, Pu<sup>240</sup>, and Pu<sup>242</sup> Sher's Systematics results are recommended. These values are expected to be fairly accurate because of the excellent agreement between the Systematics and LSQ results for the other six nuclides.

A quantity which is of great importance to the gamma energy transport calculations in Section 4 is the fraction of the energy release in the form of gamma rays. This quantity is markedly different for normal power versus LOCA conditions. In the normal power case, it is the ratio of the sum of the prompt ( $\bar{E}_{\gamma p}$ ), delayed ( $\bar{E}_{\gamma d}$ ) and capture ( $(\nu - 1)\bar{E}_{c\gamma}$ ) energy to the total energy release (Q):

$$\gamma_{np} = \frac{\bar{E}_{\gamma p} - \bar{E}_{\gamma d} + (\nu - 1)\bar{E}_{c\gamma}}{Q} \quad (2-1)$$

In the LOCA case, it is the ratio of the delayed gamma energy to the sum of the delayed beta ( $\bar{E}_{\beta}$ ) and gamma energy:

$$\gamma_{LOCA} = \frac{\bar{E}_{\gamma d}}{\bar{E}_{\gamma d} - \bar{E}_{\beta}} \quad (2-2)$$

This is, of course, the same expression as the previous one with all of the prompt sources set to zero. Table 2-12 summarizes the current and the recommended data for both normal and LOCA conditions. Values for the individual isotopes U<sup>235</sup>, U<sup>238</sup>, and Pu<sup>239</sup> are also shown. The isotope-dependent values are nearly identical for LOCA conditions, while some differences exist for the normal power case. As a result of this, the normal power value will vary somewhat with exposure. The weighted averages of the isotopic values are based on the fission fractions of the typical reload bundle 8D250 at zero exposure. These weighted average values are recommended for general use and are, in fact, utilized in Section 4. There is no approximation here in using the LOCA value. The use of the normal power value, which is far less important, may result in an error of at most 1% or 2%.

As mentioned before, the calculation of the capture gamma contribution to the energy release is a function of the type of reactor. The details of this calculation for a BWR will now be presented. The first step in the calculation is to identify the isotopes which are undergoing capture and to compute the energy release per capture. Table 2-13 is a list of the most important heavy elements, structural materials, and burnable poisons which are present in a BWR. The second column of the table gives the type of reaction which is being considered. Ordinarily this is a simple capture followed by the emission of one or more gammas which leaves the product nucleus in a stable or nearly stable state. In this case, the total energy release is easily determined by a mass balance between the product and reactant nuclei. In several cases the situation is more complicated because the product nucleus is unstable and decays by beta emission with a half-life on the order of days or less. In this case, a careful calculation of the decay energy must be made in order to exclude the energy carried away and lost by antineutrinos. Two examples of this type of calculation are presented in the next subsection and therefore the details of such calculations will be avoided here.

The third column of Table 2-13 lists the capture energy release values computed by Crowther and used in his analysis of energy per fission. The fourth column gives the new recommended values. When a beta decay calculation was performed, the value of the total beta plus gamma decay energy is also indicated. The most significant difference between the old and new values is for the U<sup>238</sup> case. Evidently, the old value inadvertently contained a contribution from antineutrino energy. The drop in energy is substantial and is the principal cause for the drop in the average beta decay energy given in Table 2-1.

The control isotope in Table 2-13 is a conglomeration of captures in control blades, fission products, and any other isotopes not explicitly given. The arbitrary choice of 5 MeV per capture is reasonable because captures in fission products will generally produce energies greater than this, compensating for the lesser amount of energy produced by an absorption in a control blade.

The next step in the calculation is to determine the relative number of captures in the various isotopes. This is clearly a function of bundle design as well as exposure. Table 2-14 gives the number of captures in each isotope per fission for three different BWR bundle designs at several different exposures. The total number of captures in each column is equal to the average number of neutrons produced per fission minus one. The total capture energy per fission is determined by multiplying the energy per capture for each isotope from Table 2-13 times the number of captures per fission from Table 2-14 and then summing over all isotopes. The average energy per capture is found by dividing this value by the total number of captures per fission ( $\nu - 1$ ). These values are shown in the bottom row of Table 2-14. Note that the average energy per capture does not appear to be strongly exposure dependent as does the capture energy per fission in the previous row. This is the primary reason for utilizing the present strategy. The average of the nine separate values for the average energy per capture is  $5.46 \pm 0.19$  MeV. This is the value which was adopted for use in the energy per fission calculations at the beginning of this subsection.

**Table 2-2**  
**ENERGY RELEASE PER FISSION OF U<sup>238</sup>**

Source:	R. L. Crowther (Aug. 1969)	Unik & Gindler (Apr. 1971)		Sher (Oct. 1976)	
		Mass Excess	Summation	LSQ	Systematics
Kinetic Energy of Fragments	168.5		165.9±2.0	[170.03±0.66]	168.4±1.5
Mass Excess		205.89±0.45		206.15±0.33	
Average Beta Energy, $\overline{E}_\beta$	7.1 <sup>a</sup>		10.5±0.6	[8.25±0.08]	8.25±0.4
Minus Antineutrinos, $-\overline{E}_\nu$		-14.7±0.9		-11.14±0.11	
Prompt Gamma Energy, $\overline{E}_{\gamma p}$	7.54 <sup>a</sup>		7.6±1.5	[6.28±0.80]	7.7±2.3
Delayed Gamma Energy, $\overline{E}_{\gamma d}$	8.0 <sup>a</sup>		9.0±1.5	[8.04±0.08]	8.0±0.4
Neutrons:					
Number released, $\nu$	2.952		2.81±0.05	2.897 <sup>b</sup>	
Average Energy, $\overline{E}_n$	2.0 <sup>a</sup>				
Total Energy, $\nu\overline{E}_n$	5.9		5.60±0.16		5.51±0.1
Minus Incident Energy, $-\overline{E}_i$	0.0		-2.8 <sup>c</sup>		-3.1±0.1
<b>Subtotal</b>	<b>197.04</b>	<b>191.2±1.0</b>	<b>195.8</b>	<b>195.01±0.34</b>	<b>194.8±1.2</b>
Capture Gammas:					
Average Energy, $\overline{E}_{c\gamma}$		6.53±0.2	6.53±0.2	5.46±0.19	5.46±0.19
Total Energy, $(\nu-1)\overline{E}_{c\gamma}$	8.58	11.82±0.5	11.82±0.5	10.36±0.36	10.36±0.36
Miscellaneous Corrections:	0.17				
<b>Total, Q</b>	<b>205.79</b>	<b>203.0±1.1</b>	<b>207.6</b>	<b>205.4±0.50</b>	<b>205.2</b>

<sup>a</sup>Estimated by Crowther  
<sup>b</sup>ENDF B-IV value with N→2N correction  
<sup>c</sup>Computed for EBR-II by Unik & Gindler

Table 2-3  
ENERGY RELEASE PER FISSION OF Pu<sup>239</sup>

Source:	R. L. Crowther (Aug. 1969)	Unik & Gindler (Apr. 1971)		Sher (Oct. 1976)	
		Mass Excess	Summation	LSQ	Systematics
Kinetic Energy of Fragments	174.8		174.0±2.0	[175.9±0.1]	176.0±1.5
Mass Excess		207.16±0.21		207.20±0.33	
Average Beta Energy, $\bar{E}_\beta$	5.58		6.3±0.3	[5.30±0.10]	5.7±0.3
Minus Antineutrinos, $-\bar{E}_\nu$		-8.8±0.5		-7.15±0.11	
Prompt Gamma Energy, $\bar{E}_{\gamma p}$	7.54 <sup>a</sup>		8.01±0.94	[7.78±0.45]	6.2±2.0
Delayed Gamma Energy, $\bar{E}_{\gamma d}$	7.0		6.8±1.5	[5.16±0.1]	5.6±0.3
Neutrons:					
Number released, $\nu$	2.89		2.880±0.009	2.873 <sup>b</sup>	
Average Energy, $\bar{E}_n$	2.0 <sup>a</sup>				
Total Energy, $\nu\bar{E}_n$	5.8		5.87±0.11		5.9±0.1
Minus Incident Energy, $-\bar{E}_i$	0.0		0.0		0.0
<b>Subtotal</b>	<b>200.72</b>	<b>198.4±0.5</b>	<b>200.98</b>	<b>200.05±0.34</b>	<b>199.4±1.5</b>
Capture Gammas:					
Average Energy, $\bar{E}_{c\gamma}$		6.53±0.2	6.53±0.2	5.46±0.19	5.46±0.19
Total Energy, $(\nu-1)\bar{E}_{c\gamma}$	8.58	12.26±0.4	12.26±0.4	10.23±0.36	10.23±0.36
Miscellaneous Corrections:	0.17				
<b>Total, Q</b>	<b>209.47</b>	<b>210.6±0.7</b>	<b>213.2</b>	<b>210.3±0.5</b>	<b>209.6</b>

<sup>a</sup>Estimated by Crowther  
<sup>b</sup>ENDF B-IV value

Table 2-4  
ENERGY RELEASE PER FISSION OF Pu<sup>241</sup>

Source:	R. L. Crowther (Aug. 1969)	Unik & Gindler (Apr. 1971)		Sher (Oct. 1976)	
		Mass Excess	Summation	LSQ	Systematics
Kinetic Energy of Fragments	174.0		175.6±2.0	[175.53±1.1]	175.5±1.5
Mass Excess		210.92±0.22		211.00±0.33	
Average Beta Energy, $\bar{E}_\beta$	7.0 <sup>a</sup>		8.2±0.4	[6.51±0.07]	7.1±0.04
Minus Antineutrinos, $-\bar{E}_\nu$		-11.5±0.7		-8.78±0.09	
Prompt Gamma Energy, $\bar{E}_{\gamma p}$	7.54 <sup>a</sup>		7.6±1.5	[7.86±1.2]	6.4±2.0
Delayed Gamma Energy, $\bar{E}_{\gamma d}$	8.0 <sup>a</sup>		7.9±1.5	[6.33±0.07]	6.7±0.4
Neutrons:					
Number released, $\nu$	3.03		2.934±0.001	2.932 <sup>b</sup>	
Average Energy, $\bar{E}_n$	2.0 <sup>a</sup>				
Total Energy, $\nu\bar{E}_n$	6.1		5.85±0.15		5.99±0.13
Minus Incident Energy, $-\bar{E}_i$	0.0		0.0		0.0
<b>Subtotal</b>	<b>202.64</b>	<b>199.4±0.7</b>	<b>205.15</b>	<b>202.22±0.33</b>	<b>201.5±1.1</b>
Capture Gammas:					
Average Energy, $\bar{E}_{c\gamma}$		6.53±0.2	6.53±0.2	5.46±0.19	5.46±0.19
Total Energy, $(\nu-1)\bar{E}_{c\gamma}$	8.58	12.63±0.4	12.63±0.4	10.55±0.37	10.55±0.37
Miscellaneous Corrections:	0.17				
<b>Total, Q</b>	<b>211.39</b>	<b>212.0±0.8</b>	<b>217.8</b>	<b>212.8±0.5</b>	<b>212.1</b>

<sup>a</sup>Estimated by Crowther  
<sup>b</sup>ENDF/B-V value

Table 2-5  
ENERGY RELEASE PER FISSION OF U<sup>233</sup>

Source:	R. L. Crowther (Aug. 1969)	Unik & Gindler (Apr. 1971)		Sher (Oct. 1976)	
		Mass Excess	Summation	LSQ	Systematics
Kinetic Energy of Fragments	169.3		167.5±2.0	[168.68±0.68]	169.5±1.5
Mass Excess		197.99±0.21		198.20±0.10	
Average Beta Energy, $\bar{E}_\beta$	7.2 <sup>a</sup>		5.6±0.3	[5.13±0.04]	5.3±0.2
Minus Antineutrinos, $-\bar{E}_\nu$		-7.8±0.5		-6.91±0.05	
Prompt Gamma Energy, $\bar{E}_{\gamma p}$	7.54 <sup>a</sup>		7.6±1.5	[7.59±0.71]	6.3±2.0
Delayed Gamma Energy, $\bar{E}_{\gamma d}$	7.0 <sup>a</sup>		5.9±1.3	[4.99±0.04]	5.1±0.2
Neutrons:					
Number released, $\nu$	2.494		2.487±0.007	2.498 <sup>b</sup>	
Average Energy, $\bar{E}_n$	1.93				
Total Energy, $\nu\bar{E}_n$	4.8	4.90±0.15		4.9±0.1	
Minus Incident Energy, $-\bar{E}_i$	0.0	0.0		0.0	
<b>Subtotal</b>	<b>195.84</b>	<b>190.2±0.5</b>	<b>191.50</b>	<b>191.29±0.11</b>	<b>191.1±1.1</b>
Capture Gammas:					
Average Energy, $\bar{E}_{c\gamma}$		6.53±0.2	6.53±0.2	5.46±0.19	5.46±0.19
Total Energy, $(\nu-1)\bar{E}_{c\gamma}$	8.58	9.71±0.3	9.71±0.3	8.18±0.28	8.18±0.28
Miscellaneous Corrections:	0.17				
<b>Total, Q</b>	<b>204.59</b>	<b>200.0±0.6</b>	<b>201.21</b>	<b>199.5±0.3</b>	<b>199.3</b>

<sup>a</sup>Estimated by Crowther  
<sup>b</sup>ENDF-B-IV value

Table 2-6  
ENERGY RELEASE PER FISSION OF Th<sup>232</sup>

Source:	R. L. Crowther (Aug. 1969)	Unik & Gindler (Apr. 1971)		Sher (Oct. 1976)	
		Mass Excess	Summation	LSQ	Systematics
Kinetic Energy of Fragments	163.2		160.0±2.0	[162.1±1.5]	162.1±1.5
Mass Excess		196.37±0.35		196.95±0.50	
Average Beta Energy, $\bar{E}_\beta$	7.5 <sup>1</sup>		9.5±0.5	[8.23±0.21]	7.8±0.4
Minus Antineutrinos, $-\bar{E}_\nu$		-13.3±0.8		-11.10±0.29	
Prompt Gamma Energy, $\bar{E}_{\gamma p}$	7.54 <sup>2</sup>		7.6±1.5	[6.15±1.75]	7.4±2.0
Delayed Gamma Energy, $\bar{E}_{\gamma d}$	8.0 <sup>3</sup>		9.0±1.5	[8.01±0.20]	7.6±0.4
Neutrons:					
Number released, $\nu$	2.746		2.36±0.07	2.699 <sup>o</sup>	
Average Energy, $\bar{E}_n$	2.0 <sup>1</sup>				
Total Energy, $\nu\bar{E}_n$	5.5		4.49±0.17		4.7±0.12
Minus Incident Energy, $-\bar{E}_i$	0.0		-3.0		-3.35±0.10
<b>Subtotal</b>	<b>191.74</b>	<b>183.1±0.9</b>	<b>187.59</b>	<b>185.85±0.58</b>	<b>186.1±1.1</b>
Capture Gammas:					
Average Energy, $\bar{E}_{c\gamma}$		6.53±0.2	6.53±0.2	5.46±0.19	5.46±0.19
Total Energy, $(\nu-1)\bar{E}_{c\gamma}$	8.58	8.88±0.5	8.88±0.5	9.28±0.32	9.28±0.32
Miscellaneous Corrections:	0.17				
<b>Total, Q</b>	<b>200.49</b>	<b>192.0±1.0</b>	<b>196.5</b>	<b>195.1±0.7</b>	<b>195.4</b>

<sup>1</sup>Estimated by Crowther  
<sup>2</sup>ENDF-B-IV value

Table 2-7  
ENERGY RELEASE PER FISSION OF U<sup>234</sup>

Source:	R. L. Crowther (Aug. 1969)		Unik & Gindler (Apr. 1971)		Sher (Oct. 1976)	
	Mass Excess	Summation	LSQ	Systematics		
Kinetic Energy of Fragments						169.4 ± 1.5
Mass Excess						
Average Beta Energy, $\bar{E}_\beta$						5.8 ± 0.3
Minus Antineutrinos, $-\bar{E}_\nu$						
Prompt Gamma Energy, $\bar{E}_{\gamma p}$						6.6 ± 2.0
Delayed Gamma Energy, $\bar{E}_{\gamma d}$						5.6 ± 0.3
Neutrons:						
Number released, $\nu$						2.371
Average Energy, $\bar{E}_n$						
Total Energy, $\nu\bar{E}_n$						5.34 ± 0.1
Minus Incident Energy, $-\bar{E}_i$						-2.36 ± 0.1
<b>Subtotal</b>	<b>NA<sup>a</sup></b>	<b>NA</b>	<b>NA</b>	<b>NA</b>	<b>NA</b>	<b>190.3 ± 1.1</b>
Capture Gammas:						
Average Energy, $\bar{E}_{c\gamma}$						5.46 ± 0.19
Total Energy, $(\nu-1)\bar{E}_{c\gamma}$						7.49 ± 0.26
Miscellaneous Corrections:						
<b>Total Q</b>						<b>197.8 ± 1.1</b>

<sup>a</sup>NA = Not available

Table 2-8  
ENERGY RELEASE PER FISSION OF U<sup>235</sup>

Source:	R. L. Crowther (Aug. 1969)		Unik & Gindler (Apr. 1971)		Sher (Oct. 1976)	
	Mass Excess	Summation	LSQ	Systematics		
Kinetic Energy of Fragments						168.9±1.5
Mass Excess						
Average Beta Energy, $\bar{E}_\beta$						7.0±0.4
Minus Antineutrinos, $-\bar{E}_\nu$						
Prompt Gamma Energy, $\bar{E}_{\gamma p}$						7.6±2.0
Delayed Gamma Energy, $\bar{E}_{\gamma d}$						6.8±0.4
Neutrons:						
Number released, $\nu$						2.464
Average Energy, $\bar{E}_n$						
Total Energy, $\nu\bar{E}_n$						5.35±0.15
Minus Incident Energy, $-\bar{E}_i$						-2.82±0.1
<b>Subtotal</b>	<b>NA<sup>a</sup></b>	<b>NA</b>	<b>NA</b>	<b>NA</b>	<b>NA</b>	<b>192.8±1.1</b>
Capture Gammas:						
Average Energy, $\bar{E}_{\gamma c}$						5.46±0.19
Total Energy, $(\nu-1)\bar{E}_{\gamma c}$						7.99±0.28
Miscellaneous Corrections:						
<b>Total Q</b>						<b>200.8±1.1</b>

<sup>a</sup>NA = Not available

Table 2-9  
ENERGY RELEASE PER FISSION OF Pu<sup>240</sup>

Source:	R. L. Crowther (Aug. 1969)	Unik & Gindler (Apr. 1971)		Sher (Oct. 1976)	
		Mass Excess	Summation	LSQ	Systematics
Kinetic Energy of Fragments					175.8±1.5
Mass Excess		206.4±1.6			
Average Beta Energy, $\overline{E}_\beta$					6.1±0.3
Minus Antineutrinos, $-\overline{E}_\nu$		-10.1±0.6			
Prompt Gamma Energy, $\overline{E}_{\gamma p}$					5.2±2.0
Delayed Gamma Energy, $\overline{E}_{\gamma d}$					6.0±0.3
Neutrons:					
Number released, $\nu$		3.17±0.20			3.177
Average Energy, $\overline{E}_n$					
Total Energy, $\nu\overline{E}_n$					6.70±0.15
Minus Incident Energy, $-\overline{E}_i$					-2.39±0.10
<b>Subtotal</b>	<b>NA<sup>a</sup></b>	<b>196.3±1.7</b>	<b>NA</b>	<b>NA</b>	<b>197.4±1.1</b>
Capture Gammas:					
Average Energy, $\overline{E}_{c\gamma}$		6.53±0.2			5.46±0.19
Total Energy, $(\nu-1)\overline{E}_{c\gamma}$		14.17±1.4			11.89±0.41
Miscellaneous Corrections:					
<b>Total Q</b>		<b>210.5±2.2</b>			<b>209.3±1.2</b>

<sup>a</sup>NA = Not available

Table 2-10  
ENERGY RELEASE PER FISSION OF Pu<sup>242</sup>

Source:	R. L. Crowther (Aug. 1969)	Unik & Gindler (Apr. 1971)		Sher (Oct. 1976)	
		Mass Excess	Summation	LSQ	Systematics
Kinetic Energy of Fragments					175.2±1.5
Mass Excess		210.8±3.2			
Average Beta Energy, $\bar{E}_\beta$					7.4±0.4
Minus Antineutrinos, $-\bar{E}_\nu$		-12.9±0.8			
Prompt Gamma Energy, $\bar{E}_{\gamma p}$					6.5±2.2
Delayed Gamma Energy, $\bar{E}_{\gamma d}$					7.2±0.4
Neutrons:					
Number released, $\nu$		3.18±0.40			3.138
Average Energy, $\bar{E}_n$					
Total Energy, $\nu\bar{E}_n$					6.50±0.15
Minus Incident Energy, $-\bar{E}_i$					-2.32±0.1
<b>Subtotal</b>	<b>NA<sup>a</sup></b>	<b>197.9±3.3</b>	<b>NA</b>	<b>NA</b>	<b>200.6±1.1</b>
Capture Gammas:					
Average Energy, $\bar{E}_{c\gamma}$		6.53±0.2			5.46±0.19
Total Energy, $(\nu-1)\bar{E}_{c\gamma}$		14.24±2.6			11.67±0.41
Miscellaneous Corrections:					
<b>Total Q</b>		<b>212.1±4.2</b>			<b>212.3±1.2</b>

<sup>a</sup>NA = Not available

**Table 2-11**  
**SUMMARY OF CURRENT AND RECOMMENDED VALUES FOR ENERGY RELEASE PER FISSION**

Nuclide	Q Current- GEBLA05 (MeV/fission)	Q Recommended (MeV/fission)
U <sup>235</sup>	204.4	201.8
U <sup>238</sup>	205.8	205.4
Pu <sup>239</sup>	209.5	210.3
Pu <sup>241</sup>	211.4	212.8
U <sup>233</sup>	198.0	199.5
Th <sup>232</sup>	197.0	195.1
U <sup>234</sup>	205.8	197.8
U <sup>236</sup>	205.8	200.8
Pu <sup>240</sup>	205.8	209.3
Pu <sup>242</sup>	205.8	212.3

**Table 2-12**  
**FRACTIONAL ENERGY RELEASE PER FISSION IN THE FORM OF GAMA RAYS**

	Nuclide	Normal Power	LOCA
Current (Scatena & Upham, Dec. 1973)	All	0.111	0.47
LSQ (Sher, Dec. 1976)	U <sup>235</sup>	0.104	0.493
LSQ (Sher, Dec. 1976)	U <sup>238</sup>	0.120	0.494
LSQ (Sher, Dec. 1976)	Pu <sup>239</sup>	0.110	0.493
Recommended-Weighted Average		0.105	0.493

Table 2-13  
ENERGY RELEASE PER CAPTURE IN SELECTED ISOTOPES

Isotope	Reaction	R. L. Crowther (MeV/Capture)	Recommended (MeV/Capture)
U <sup>235</sup>	(n,γ)U <sup>236</sup>	6.54	6.54
U <sup>236</sup>	(n,γ)U <sup>237</sup> (,β <sup>-</sup> )Np <sup>237</sup>	5.93	5.12 - C.35 = 5.47
U <sup>238</sup>	(n,γ)U <sup>239</sup> (,β <sup>-</sup> )Np <sup>239</sup> (,β <sup>-</sup> )Pu <sup>239</sup>	4.80 - 1.28 - 0.72 = 6.80	4.80 + 0.46 + C.42 = 5.68
Np <sup>237</sup>	(n,γ)Np <sup>238</sup> (,β <sup>-</sup> )Pu <sup>238</sup>	6.67	5.48 - C.46 = 5.94
Np <sup>239</sup>	(n,γ)Np <sup>240</sup> (,β <sup>-</sup> )Pu <sup>240</sup>	6.10	5.15 - 0.75 - 0.42 <sup>a</sup> = 5.48
Pu <sup>239</sup>	(n,γ)Pu <sup>240</sup>	6.39	6.53
Pu <sup>240</sup>	(n,γ)Pu <sup>241</sup>	5.83	5.24
Pu <sup>241</sup>	(n,γ)Pu <sup>242</sup>	6.02	6.30
Pu <sup>242</sup>	(n,γ)Pu <sup>243</sup> (,β <sup>-</sup> )Am <sup>243</sup>	5.46	5.04 - C.18 = 5.22
Am <sup>241</sup>	(n,γ)Am <sup>242</sup> (,β <sup>-</sup> )Cm <sup>242</sup>	6.11	5.52 - C.23 = 5.75
Am <sup>243</sup>	(n,γ)Am <sup>244</sup> (,β <sup>-</sup> )Cm <sup>244</sup>	6.67	5.34 - C.48 = 5.82
Pu <sup>238</sup>	(n,γ)Pu <sup>239</sup>	5.55	5.65
Cm <sup>244</sup>	(n,γ)Cm <sup>245</sup>	5.83	5.52
H <sup>1</sup>	(n,γ)H <sup>2</sup>	2.22	2.22
Zr <sup>90</sup>	(n,γ)Zr <sup>91</sup>	7.19	7.20
Zr <sup>91</sup>	(n,γ)Zr <sup>92</sup>	8.64	8.63
Zr <sup>92</sup>	(n,γ)Zr <sup>93</sup>	6.72	6.76
Zr <sup>94</sup>	(n,γ)Zr <sup>95</sup> (,β <sup>-</sup> )Nb <sup>95</sup> (,β <sup>-</sup> )Mo <sup>95</sup>	6.47	6.47 - 0.84 - C.81 = 8.12
Zr <sup>96</sup>	(n,γ)Zr <sup>97</sup> (,β <sup>-</sup> )Nb <sup>97</sup> (,β <sup>-</sup> )Mo <sup>97</sup>	5.58	5.57 - 1.51 - 1.13 = 8.21
Zr - 2		7.91	8.16
B <sup>10</sup>	(n,γ)Li <sup>7</sup>	2.79	2.79
Gd <sup>155</sup>	(n,γ)Gd <sup>156</sup>	8.52	8.53
Gd <sup>157</sup>	(n,γ)Gd <sup>158</sup>	7.93	7.93
O <sup>16</sup>	(n,γ)O <sup>17</sup>	4.14	4.14
Control		5	5

<sup>a</sup>The decay energy of Np<sup>239</sup> is subtracted since all captures in U<sup>238</sup> were assumed to lead to a decay of Np<sup>239</sup>.

Table 2-14  
NEUTRON CAPTURE RATES AND AVERAGE ENERGY RELEASE  
PER CAPTURE FOR TYPICAL FUEL DESIGNS

Bundle: Exposure (GWd/t):	TVA			2.33-4Gd(.04)		8D250			
	0.0	12.5	25.0	0.0	9.0	0.0	10.0	20.0	30.0
Captures per Fission for:									
U <sup>235</sup>	0.2048	0.1183	0.06919	0.2013	0.1275	0.21449	0.13165	0.08675	0.05304
U <sup>236</sup>	0.0	0.01127	0.01842	0.0	0.00917	0.00109	0.01401	0.02209	0.02875
U <sup>238</sup>	0.5596	0.6145	0.7343	0.6038	0.6322	0.62554	0.65304	0.70684	0.80056
Np <sup>237</sup>	0.0	0.0035	0.01046	0.0	0.00217	0.0	0.00374	0.01033	0.01882
Np <sup>239</sup>	0.0	0.00024	0.00033	0.0	0.00026	0.0	0.00021	0.00025	0.00034
Pu <sup>239</sup>	0.0	0.1925	0.2639	0.0	0.1714	0.0	0.17645	0.23993	0.27867
Pu <sup>240</sup>	0.0	0.1036	0.1930	0.0	0.07864	0.0	0.08716	0.16097	0.22545
Pu <sup>241</sup>	0.0	0.01419	0.03833	0.0	0.00898	0.0	0.00988	0.02766	0.4586
Pu <sup>242</sup>	0.0	0.00135	0.00774	0.0	0.00064	0.0	0.00091	0.00563	0.01514
Am <sup>241</sup>	0.0	0.00125	0.00454	0.0	0.00039	0.0	0.00092	0.00400	0.00707
Am <sup>243</sup>	0.0	0.00013	0.00182	0.0	0.00005	0.0	0.00008	0.00106	0.00450
Pu <sup>238</sup>	0.0	0.00085	0.00576	0.0	0.00031	0.0	0.00069	0.00417	0.01171
Cm <sup>244</sup>	0.0	0.0	0.00014	0.0	0.0	0.0	0.0	0.00008	0.00050
H <sup>1</sup>	0.1742	0.1949	0.2599	0.1564	0.1567	0.14971	0.14960	0.17570	0.20181
Zr-2	0.03433	0.03812	0.04712	0.05893	0.06097	0.04636	0.04831	0.05340	0.06092
Gd <sup>155</sup>	0.0	0.0	0.0	0.05049	0.00447	0.04498	0.00024	0.00044	0.00070
Gd <sup>157</sup>	0.0	0.0	0.0	0.1864	0.00407	0.15599	0.00103	0.00133	0.00179
O <sup>16</sup>	0.0031	0.00337	0.00377	0.00380	0.00405	0.00383	0.00409	0.00430	0.00486
Control <sup>a</sup>	0.4901	0.1700	0.0	0.1920	0.3503	0.23026	0.35589	0.25369	0.34826
Total $\left(\frac{\nu-1}{k_x}\right)$	1.4661	1.4681	1.6587	1.4533	1.6120	1.4725	1.6371	1.7586	2.1088
Total Capture Energy per Fission:	7.647	7.864	8.850	8.457	8.767	8.459	8.887	9.558	11.395
Average Energy per Capture:	5.22	5.36	5.34	5.82	5.44	5.74	5.43	5.43	5.40
Average of All Cases:									5.46 ± .19

<sup>a</sup> Includes 1/v absorber, fission products, and other isotopes not listed.

2.2 DECAY PARAMETERS OF THE ACTINIDES

The two most important actinides for ECCS analyses in low-enriched light water reactors are U<sup>239</sup> and Np<sup>239</sup>. All other actinides have such long half-lives or exist in such low concentrations that their decay energies are insignificant.

The half-lives and beta disintegration energies of U<sup>239</sup> and Np<sup>239</sup> have been taken from the *Table of Isotopes*<sup>9</sup>. They are listed in Tables 2-15 and 2-16. Also present in these tables are details of the various decay modes of each isotope, taken from the same reference. For each decay mode, with a probability greater than 0.1%, the transition probability is given along with the type of transition, the gamma energy and the maximum beta energy. The ratio of the average beta energy to the maximum energy has been taken from the tables of Widman<sup>10</sup>. This quantity is a function of the maximum beta energy and the charge number of the daughter nucleus. The right-hand column in Tables 2-15 and 2-16 contains the average beta energy for the given transition. The gamma energy plus the average beta energy for each transition is weighted by the transition probability and summed over all transitions. The resulting quantity is the total sensible energy release through beta decay.

A summary of the old and new values for the sensible beta decay energies of U<sup>239</sup> and Np<sup>239</sup> are presented in Table 2-17. The first row gives the values currently in use for ECCS calculations. The second row gives the values in the ANS5.1 subcommittee's draft for a new decay heat standard<sup>4</sup>. The bottom row gives the values which are recommended for use.

Table 2-15  
BETA DECAY PROPERTIES OF U<sup>239</sup>

Half Life =  $\tau_{1/2} = 23.5$  min.  
Decay Constant =  $\lambda = 4.91 \times 10^{-4}$  sec<sup>-1</sup>  
Beta Disintegration Energy =  $Q_{\beta} = 1.28$  MeV

Beta Decay Modes:

Transition Probability	Type of Transition	Gamma Energy (MeV)	Maximum Beta Energy, E (MeV)	Average/Maximum Energy (MeV)	Average Beta Energy, $\bar{E}$ (MeV)
0.80	Non-Unique 1st Forbidden	0.07467	1.21	0.329	0.398
0.20	Allowed	0.0	1.28	0.332	0.425
Average		0.060			0.403

Total Sensible Energy Release = 0.463 MeV

Table 2-16  
BETA DECAY PROPERTIES OF Np<sup>239</sup>

Half Life =  $\tau_{1/2}$  = 2.35 days  
 Decay Constant =  $\lambda$  =  $3.41 \times 10^{-6}$  sec<sup>-1</sup>  
 Beta Disintegration Energy =  $Q_{\beta^-}$  = 0.723 MeV

Beta Decay Modes:

Transition Probability <sup>a</sup>	Type of Transition	Gamma Energy (MeV)	Maximum Beta Energy, E (MeV)	Average/Maximum Energy (MeV)	Average Beta Energy, $\bar{E}$ (MeV)
0.01	Allowed	0.512	0.211	0.272	0.057
0.32	Non-Unique 1st forbidden	0.392	0.331	0.282	0.093
0.07	Allowed	0.330	0.393	0.286	0.112
0.48	Allowed	0.286	0.437	0.289	0.126
0.05 <sup>b</sup>	Allowed	0.076	0.647	0.302	0.195
	Allowed	0.057	0.666	0.303	0.202
0.07	Allowed	0.008	0.715	0.306	0.219
Average		0.295			0.124

Total Sensible Energy Release = 0.419 MeV

<sup>a</sup> Transitions with probabilities less than 0.1% have been ignored.

<sup>b</sup> Each of these two transitions is assumed to be equally likely, i.e. to have a transition probability of 0.025.

Table 2-17  
COMPARISON OF OLD AND NEW VALUES FOR THE SENSIBLE BETA DECAY ENERGIES OF U<sup>239</sup> AND Np<sup>239</sup>

	$E_{\beta_1}$ (MeV)	$E_{\beta_2}$ (MeV)
	U <sub>239</sub>	Np <sub>239</sub>
Current Value	0.456	0.434
Draft ANS-5.1	0.474	0.419
Recommended	0.463	0.419

### 3. NUCLEAR ENERGY SOURCES

Subsection 3.1 of this section is concerned with the identification and quantification of all possible nuclear sources of heat in a nuclear reactor during a loss-of-coolant accident (LOCA). Subsection 3.2 is a series of specifications for combining these sources of heat into decay heat curves for use in ECCS analyses. Three decay heat models will be considered. The first is the model currently in use<sup>11</sup>. The second is an improvement of the current model which is still consistent with the current ANS-5 decay heat standard<sup>2,3</sup>. The third and final model is a more elaborate method which is based on the ANS-5.1 subcommittee's draft of a proposed new standard<sup>4</sup>.

#### 3.1 EVALUATION OF ENERGY SOURCES

There are four potential nuclear energy sources in a reactor following shutdown: decay heat from fission products, decay heat from actinides, fission heat induced by delayed neutrons, and decay heat from structural materials. Each of these energy sources will be considered in a separate subsection.

##### 3.1.1 Decay Heat from Fission Products

The decay heat from fission products may be evaluated either from an experiment or through a calculation based on fission yields and decay data. In either case, the results consist of the power (MeV per second) as a function of time after shutdown divided by the fission rate (fissions per second) prior to shutdown. In order to relate this to a meaningful quantity for ECCS analysis, such as the ratio of the power as a function of time to the initial power, it is necessary to divide the experimental or calculated curves by  $\bar{Q}$ , the average energy per fission prior to shutdown. This has the effect of relating the decay heat per fission to the actual fission rate in the reactor.

The current standard for decay heat which is used for ECCS calculations was formulated by the ANS-5 subcommittee of the ANS Standards Committee<sup>2,3</sup>. This standard, which will be referred to hereafter as the ANS-5 standard, is reproduced in Table 3-1. The first column of this table is the time in seconds after shutdown. This is followed by the relative power  $P(t)/P(0)$  in column two. The relative power was computed by the standards subcommittee by arbitrarily assuming that  $\bar{Q}$  was equal to 200 MeV/fission. However, as it was pointed out in Section 2,  $\bar{Q}$  is not exactly equal to this value, and in fact it is a function of the exposure of the reactor fuel. In order to produce a more realistic decay heat curve it is therefore necessary to remove the arbitrary factor of 200 MeV/fission. In column three of Table 3-1, the ANS-5 standard has been converted to the more rational MeV per fission curve by multiplying the relative power by 200 MeV/fission. This decay heat curve will be denoted by  $D_s(t, \infty)$  where  $t$  is the time in seconds after shutdown and the argument  $\infty$  denotes that the curve assumes an infinite reactor operating time.

The ANS-5 standard is currently under review for possible revision. The ANS-5.1 subcommittee has released a draft of a proposed new standard<sup>4</sup>. This new standard recognizes that the decay heat produced by different fissionable isotopes is significantly different and therefore provides separate curves for the isotopes  $U^{235}$ ,  $U^{238}$ , and  $Pu^{239}$ . These curves are reproduced in Tables 3-2, 3-3, and 3-4, respectively. The notation  $D_{pi}(t, \infty)$  is used to denote the decay heat in units of MeV per fission for isotope  $i$  at  $t$  seconds after shutdown. The reactor operating time is assumed to be infinite as before. The index  $i$  equal to 1 represents  $U^{235}$  while values of 2 and 3 are used for  $U^{238}$  and  $Pu^{239}$ , respectively.

##### 3.1.2 Decay Heat from Actinides

There are only two actinides which are of importance to decay heat calculations in low-enriched light water reactors:  $U^{239}$  and  $Np^{239}$ . All other actinides have such low densities or long half-lives that their contribution to decay heat is completely negligible. What follows is a straightforward derivation of the contribution of  $U^{239}$  and  $Np^{239}$  to decay heat.

Table 3-1  
 TABULAR DATA FOR THE ANS-5 (OCTOBER 1973) STANDARD DECAY HEAT POWER FOR INFINITE REACTOR OPERATING TIME

Time After Shutdown, t(sec)	Relative Power, P(t)/P(0)	Decay Heat, $D_5(t, \infty)$ (MeV/fission)	Time After Shutdown, t(sec)	Relative Power, P(t)/P(0)	Decay Heat, $D_5(t, \infty)$ (MeV/fission)
$1 \times 10^{-1}$	$6.75 \times 10^{-2}$	$1.350 \times 10^1$	$6 \times 10^4$	$5.66 \times 10^{-3}$	$1.132 \times 10^0$
$1 \times 10^0$	$6.25 \times 10^{-2}$	$1.250 \times 10^1$	$8 \times 10^4$	$5.05 \times 10^{-3}$	$1.010 \times 10^0$
$2 \times 10^0$	$5.90 \times 10^{-2}$	$1.180 \times 10^1$	$1 \times 10^5$	$4.75 \times 10^{-3}$	$9.500 \times 10^{-1}$
$4 \times 10^0$	$5.52 \times 10^{-2}$	$1.104 \times 10^1$	$2 \times 10^5$	$4.00 \times 10^{-3}$	$8.000 \times 10^{-1}$
$6 \times 10^0$	$5.33 \times 10^{-2}$	$1.066 \times 10^1$	$4 \times 10^5$	$3.39 \times 10^{-3}$	$6.780 \times 10^{-1}$
$8 \times 10^0$	$5.12 \times 10^{-2}$	$1.024 \times 10^1$	$6 \times 10^5$	$3.10 \times 10^{-3}$	$6.200 \times 10^{-1}$
$1 \times 10^1$	$5.00 \times 10^{-2}$	$1.000 \times 10^1$	$8 \times 10^5$	$2.82 \times 10^{-3}$	$5.640 \times 10^{-1}$
$2 \times 10^1$	$4.50 \times 10^{-2}$	$9.000 \times 10^0$	$1 \times 10^6$	$2.67 \times 10^{-3}$	$5.340 \times 10^{-1}$
$4 \times 10^1$	$3.96 \times 10^{-2}$	$7.920 \times 10^0$	$2 \times 10^6$	$2.15 \times 10^{-3}$	$4.300 \times 10^{-1}$
$6 \times 10^1$	$3.65 \times 10^{-2}$	$7.300 \times 10^0$	$4 \times 10^6$	$1.66 \times 10^{-3}$	$3.320 \times 10^{-1}$
$8 \times 10^1$	$3.46 \times 10^{-2}$	$6.920 \times 10^0$	$6 \times 10^6$	$1.43 \times 10^{-3}$	$2.360 \times 10^{-1}$
$1 \times 10^2$	$3.31 \times 10^{-2}$	$6.620 \times 10^0$	$8 \times 10^6$	$1.30 \times 10^{-3}$	$2.600 \times 10^{-1}$
$2 \times 10^2$	$2.75 \times 10^{-2}$	$5.500 \times 10^0$	$1 \times 10^7$	$1.17 \times 10^{-3}$	$2.340 \times 10^{-1}$
$4 \times 10^2$	$2.35 \times 10^{-2}$	$4.700 \times 10^0$	$2 \times 10^7$	$8.90 \times 10^{-4}$	$1.780 \times 10^{-1}$
$6 \times 10^2$	$2.11 \times 10^{-2}$	$4.220 \times 10^0$	$4 \times 10^7$	$6.60 \times 10^{-4}$	$1.360 \times 10^{-1}$
$8 \times 10^2$	$1.96 \times 10^{-2}$	$3.920 \times 10^0$	$6 \times 10^7$	$6.20 \times 10^{-4}$	$1.240 \times 10^{-1}$
$1 \times 10^3$	$1.85 \times 10^{-2}$	$3.700 \times 10^0$	$8 \times 10^7$	$5.70 \times 10^{-4}$	$1.140 \times 10^{-1}$
$2 \times 10^3$	$1.57 \times 10^{-2}$	$3.140 \times 10^0$	$1 \times 10^8$	$5.50 \times 10^{-4}$	$1.100 \times 10^{-1}$
$4 \times 10^3$	$1.28 \times 10^{-2}$	$2.560 \times 10^0$	$2 \times 10^8$	$4.85 \times 10^{-4}$	$9.700 \times 10^{-2}$
$6 \times 10^3$	$1.12 \times 10^{-2}$	$2.240 \times 10^0$	$4 \times 10^8$	$4.15 \times 10^{-4}$	$8.300 \times 10^{-2}$
$8 \times 10^3$	$1.05 \times 10^{-2}$	$2.100 \times 10^0$	$6 \times 10^8$	$3.60 \times 10^{-4}$	$7.200 \times 10^{-2}$
$1 \times 10^4$	$9.65 \times 10^{-3}$	$1.930 \times 10^0$	$8 \times 10^8$	$3.03 \times 10^{-4}$	$6.060 \times 10^{-2}$
$2 \times 10^4$	$7.95 \times 10^{-3}$	$1.590 \times 10^0$	$1 \times 10^9$	$2.67 \times 10^{-4}$	$5.340 \times 10^{-2}$
$4 \times 10^4$	$6.25 \times 10^{-3}$	$1.250 \times 10^0$			

Table 3-2  
 PROPOSED (ANS-5.1) TABULAR DATA FOR STANDARD DECAY HEAT POWER FOR THERMAL FISSION  
 OF  $U^{235}$  AND FOR IRRADIATION OF  $1 \times 10^{13}$  SEC

Time After Shutdown, t(sec)	Decay Heat Power, $D_{pi}(t, \infty)$ (MeV/fission) <sup>a</sup>	One Sigma Uncertainty $D_{pi}(t, \infty)$ (MeV/fission) <sup>a</sup>	Percent Uncertainty
$1.0000 \times 10^0$	$1.231 \times 10^1$	$0.040 \times 10^1$	3.3
$1.5000 \times 10^0$	$1.198 \times 10^1$	$0.032 \times 10^1$	2.7
$2.0000 \times 10^0$	$1.169 \times 10^1$	$0.028 \times 10^1$	2.4
$4.0000 \times 10^0$	$1.083 \times 10^1$	$0.023 \times 10^1$	2.2
$6.0000 \times 10^0$	$1.026 \times 10^1$	$0.021 \times 10^1$	2.1
$8.0000 \times 10^0$	$9.830 \times 10^0$	$0.198 \times 10^0$	2.0
$1.0000 \times 10^1$	$9.494 \times 10^0$	$0.187 \times 10^0$	2.0
$1.5000 \times 10^1$	$8.882 \times 10^0$	$0.170 \times 10^0$	1.9
$2.0000 \times 10^1$	$8.455 \times 10^0$	$0.159 \times 10^0$	1.9
$4.0000 \times 10^1$	$7.459 \times 10^0$	$0.137 \times 10^0$	1.8
$6.0000 \times 10^1$	$6.888 \times 10^0$	$0.125 \times 10^0$	1.8
$8.0000 \times 10^1$	$6.493 \times 10^0$	$0.118 \times 10^0$	1.8
$1.0000 \times 10^2$	$6.198 \times 10^0$	$0.112 \times 10^0$	1.8
$1.5000 \times 10^2$	$5.696 \times 10^0$	$0.103 \times 10^0$	1.8
$2.0000 \times 10^2$	$5.369 \times 10^0$	$0.097 \times 10^0$	1.8
$4.0000 \times 10^2$	$4.667 \times 10^0$	$0.083 \times 10^0$	1.8
$6.0000 \times 10^2$	$4.282 \times 10^0$	$0.076 \times 10^0$	1.8
$8.0000 \times 10^2$	$4.009 \times 10^0$	$0.071 \times 10^0$	1.8
$1.0000 \times 10^3$	$3.796 \times 10^0$	$0.067 \times 10^0$	1.8
$1.5000 \times 10^3$	$3.408 \times 10^0$	$0.060 \times 10^0$	1.8
$2.0000 \times 10^3$	$3.137 \times 10^0$	$0.055 \times 10^0$	1.8
$4.0000 \times 10^3$	$2.534 \times 10^0$	$0.045 \times 10^0$	1.8
$6.0000 \times 10^3$	$2.234 \times 10^0$	$0.039 \times 10^0$	1.7
$8.0000 \times 10^3$	$2.044 \times 10^0$	$0.036 \times 10^0$	1.7
$1.0000 \times 10^4$	$1.908 \times 10^0$	$0.033 \times 10^0$	1.7
$1.5000 \times 10^4$	$1.685 \times 10^0$	$0.030 \times 10^0$	1.8
$2.0000 \times 10^4$	$1.545 \times 10^0$	$0.027 \times 10^0$	1.8
$4.0000 \times 10^4$	$1.258 \times 10^0$	$0.023 \times 10^0$	1.9
$6.0000 \times 10^4$	$1.117 \times 10^0$	$0.021 \times 10^0$	1.9
$8.0000 \times 10^4$	$1.030 \times 10^0$	$0.020 \times 10^0$	2.0

Table 3-2 (Continued)  
 PROPOSED (ANS-5.1) TABULAR DATA FOR STANDARD DECAY HEAT POWER FOR THERMAL FISSION  
 OF  $U^{235}$  AND FOR IRRADIATION OF  $1 \times 10^{13}$  SEC

Time After Shutdown, t(sec)	Decay Heat Power, $D_p(t, \infty)$ (MeV/fission) <sup>a</sup>	One Sigma Uncertainty $D_{p1}(t, \infty)$ (MeV/fission) <sup>a</sup>	Percent Uncertainty
$1.0000 \times 10^5$	$9.691 \times 10^{-1}$	$0.194 \times 10^{-1}$	2.0
$1.5000 \times 10^5$	$8.734 \times 10^{-1}$	$0.175 \times 10^{-1}$	2.0
$2.0000 \times 10^5$	$8.154 \times 10^{-1}$	$0.163 \times 10^{-1}$	2.0
$4.0000 \times 10^5$	$6.975 \times 10^{-1}$	$0.140 \times 10^{-1}$	2.0
$6.0000 \times 10^5$	$6.331 \times 10^{-1}$	$0.127 \times 10^{-1}$	2.0
$8.0000 \times 10^5$	$5.868 \times 10^{-1}$	$0.117 \times 10^{-1}$	2.0
$1.0000 \times 10^6$	$5.509 \times 10^{-1}$	$0.110 \times 10^{-1}$	2.0
$1.5000 \times 10^6$	$4.866 \times 10^{-1}$	$0.097 \times 10^{-1}$	2.0
$2.0000 \times 10^6$	$4.425 \times 10^{-1}$	$0.089 \times 10^{-1}$	2.0
$4.0000 \times 10^6$	$3.457 \times 10^{-1}$	$0.069 \times 10^{-1}$	2.0
$6.0000 \times 10^6$	$2.983 \times 10^{-1}$	$0.060 \times 10^{-1}$	2.0
$8.0000 \times 10^6$	$2.680 \times 10^{-1}$	$0.054 \times 10^{-1}$	2.0
$1.0000 \times 10^7$	$2.457 \times 10^{-1}$	$0.049 \times 10^{-1}$	2.0
$1.5000 \times 10^7$	$2.078 \times 10^{-1}$	$0.042 \times 10^{-1}$	2.0
$2.0000 \times 10^7$	$1.846 \times 10^{-1}$	$0.037 \times 10^{-1}$	2.0
$4.0000 \times 10^7$	$1.457 \times 10^{-1}$	$0.029 \times 10^{-1}$	2.0
$6.0000 \times 10^7$	$1.308 \times 10^{-1}$	$0.026 \times 10^{-1}$	2.0
$8.0000 \times 10^7$	$1.222 \times 10^{-1}$	$0.024 \times 10^{-1}$	2.0
$1.0000 \times 10^8$	$1.165 \times 10^{-1}$	$0.023 \times 10^{-1}$	2.0
$1.5000 \times 10^8$	$1.082 \times 10^{-1}$	$0.022 \times 10^{-1}$	2.0
$2.0000 \times 10^8$	$1.032 \times 10^{-1}$	$0.021 \times 10^{-1}$	2.0
$4.0000 \times 10^8$	$8.836 \times 10^{-2}$	$0.177 \times 10^{-2}$	2.0
$6.0000 \times 10^8$	$7.613 \times 10^{-2}$	$0.152 \times 10^{-2}$	2.0
$8.0000 \times 10^8$	$6.570 \times 10^{-2}$	$0.131 \times 10^{-2}$	2.0
$1.0000 \times 10^9$	$5.678 \times 10^{-2}$	$0.114 \times 10^{-2}$	2.0

<sup>a</sup>MeV/fission is a contraction of  $\frac{\text{MeV/s}}{\text{fission}\cdot\text{s}}$

<sup>b</sup>Data for t greater than  $10^4$  are provided solely for use in Equations 3.45 and 3.46. They are not to be interpreted as standard decay heat values at these times.

Table 3-3  
 PROPOSED (ANS-5.1)  
 TABULAR DATA FOR STANDARD DECAY HEAT POWER FOR FAST FISSION OF U<sup>238</sup> AND FOR  
 IRRADIATION OF 10<sup>13</sup> SEC

Time After Shutdown, t(sec)	Decay Heat Power, D <sub>p2</sub> (t,∞) (MeV/fission) <sup>a</sup>	One Sigma Uncertainty, D <sub>p2</sub> (t,∞) (MeV/fission)	Percent Uncertainty
1.0×10 <sup>0</sup>	1.419×10 <sup>1</sup>	0.176×10 <sup>1</sup>	12.0
1.5×10 <sup>0</sup>	1.361×10 <sup>1</sup>	0.164×10 <sup>1</sup>	12.0
2.0×10 <sup>0</sup>	1.316×10 <sup>1</sup>	0.154×10 <sup>1</sup>	12.0
4.0×10 <sup>0</sup>	1.196×10 <sup>1</sup>	0.130×10 <sup>1</sup>	11.0
6.0×10 <sup>0</sup>	1.123×10 <sup>1</sup>	0.115×10 <sup>1</sup>	10.0
8.0×10 <sup>0</sup>	1.070×10 <sup>1</sup>	0.105×10 <sup>1</sup>	9.9
1.0×10 <sup>1</sup>	1.029×10 <sup>1</sup>	0.098×10 <sup>1</sup>	9.5
1.5×10 <sup>1</sup>	9.546×10 <sup>0</sup>	0.855×10 <sup>0</sup>	9.0
2.0×10 <sup>1</sup>	9.012×10 <sup>0</sup>	0.758×10 <sup>0</sup>	8.4
4.0×10 <sup>1</sup>	7.755×10 <sup>0</sup>	0.560×10 <sup>0</sup>	7.2
6.0×10 <sup>1</sup>	7.052×10 <sup>0</sup>	0.463×10 <sup>0</sup>	6.6
8.0×10 <sup>1</sup>	6.572×10 <sup>0</sup>	0.405×10 <sup>0</sup>	6.2
1.0×10 <sup>2</sup>	6.217×10 <sup>0</sup>	0.367×10 <sup>0</sup>	5.9
1.5×10 <sup>2</sup>	5.621×10 <sup>0</sup>	0.317×10 <sup>0</sup>	5.6
2.0×10 <sup>2</sup>	5.241×10 <sup>0</sup>	0.281×10 <sup>0</sup>	5.4
4.0×10 <sup>2</sup>	4.464×10 <sup>0</sup>	0.229×10 <sup>0</sup>	5.1
6.0×10 <sup>2</sup>	4.072×10 <sup>0</sup>	0.205×10 <sup>0</sup>	5.0
8.0×10 <sup>2</sup>	3.804×10 <sup>0</sup>	0.189×10 <sup>0</sup>	5.0
1.0×10 <sup>3</sup>	3.598×10 <sup>0</sup>	0.177×10 <sup>0</sup>	4.9
1.5×10 <sup>3</sup>	3.220×10 <sup>0</sup>	0.157×10 <sup>0</sup>	4.9
2.0×10 <sup>3</sup>	2.954×10 <sup>0</sup>	0.142×10 <sup>0</sup>	4.8
4.0×10 <sup>3</sup>	2.366×10 <sup>0</sup>	0.111×10 <sup>0</sup>	4.7
6.0×10 <sup>3</sup>	2.078×10 <sup>0</sup>	0.095×10 <sup>0</sup>	4.6
8.0×10 <sup>3</sup>	1.901×10 <sup>0</sup>	0.085×10 <sup>0</sup>	4.5
1.0×10 <sup>4</sup>	1.777×10 <sup>0</sup>	0.078×10 <sup>0</sup>	4.4
1.5×10 <sup>4</sup>	1.578×10 <sup>0</sup>	0.068×10 <sup>0</sup>	4.3
2.0×10 <sup>4</sup>	1.455×10 <sup>0</sup>	0.061×10 <sup>0</sup>	4.2
4.0×10 <sup>4</sup>	1.204×10 <sup>0</sup>	0.049×10 <sup>0</sup>	4.1
6.0×10 <sup>4</sup>	1.077×10 <sup>0</sup>	0.043×10 <sup>0</sup>	4.0
8.0×10 <sup>4</sup>	9.955×10 <sup>-1</sup>	0.392×10 <sup>-1</sup>	3.9

**Table 3-3 (Continued)**  
**PROPOSED (ANS-5.1)**  
**TABULAR DATA FOR STANDARD DECAY HEAT POWER FOR FAST FISSION OF U<sup>238</sup> AND FOR IRRADIATION OF 10<sup>13</sup> SEC**

Time After Shutdown t(sec)	Decay Heat Power, D <sub>p2</sub> (t <sup>∞</sup> ) (MeV/fission <sup>a</sup> )	One Sigma Uncertainty D <sub>p2</sub> (t <sup>∞</sup> ) (MeV/fission)	Percent Uncertainty
1.0 × 10 <sup>5</sup>	9.383 × 10 <sup>-1</sup>	0.366 × 10 <sup>-1</sup>	3.9
1.5 × 10 <sup>5</sup>	8.459 × 10 <sup>-1</sup>	0.327 × 10 <sup>-1</sup>	3.9
2.0 × 10 <sup>5</sup>	7.884 × 10 <sup>-1</sup>	0.303 × 10 <sup>-1</sup>	3.8
4.0 × 10 <sup>5</sup>	6.673 × 10 <sup>-1</sup>	0.258 × 10 <sup>-1</sup>	3.9
6.0 × 10 <sup>5</sup>	6.002 × 10 <sup>-1</sup>	0.233 × 10 <sup>-1</sup>	3.9
8.0 × 10 <sup>5</sup>	5.530 × 10 <sup>-1</sup>	0.216 × 10 <sup>-1</sup>	3.9
1.0 × 10 <sup>6</sup>	5.171 × 10 <sup>-1</sup>	0.204 × 10 <sup>-1</sup>	3.9
1.5 × 10 <sup>6</sup>	4.544 × 10 <sup>-1</sup>	0.180 × 10 <sup>-1</sup>	4.0
2.0 × 10 <sup>6</sup>	4.125 × 10 <sup>-1</sup>	0.165 × 10 <sup>-1</sup>	4.0
4.0 × 10 <sup>6</sup>	3.224 × 10 <sup>-1</sup>	0.132 × 10 <sup>-1</sup>	4.1
6.0 × 10 <sup>6</sup>	2.784 × 10 <sup>-1</sup>	0.117 × 10 <sup>-1</sup>	4.2
8.0 × 10 <sup>6</sup>	2.503 × 10 <sup>-1</sup>	0.107 × 10 <sup>-1</sup>	4.3
1.0 × 10 <sup>7</sup>	2.296 × 10 <sup>-1</sup>	0.101 × 10 <sup>-1</sup>	4.4
1.5 × 10 <sup>7</sup>	1.941 × 10 <sup>-1</sup>	0.086 × 10 <sup>-1</sup>	4.4
2.0 × 10 <sup>7</sup>	1.717 × 10 <sup>-1</sup>	0.076 × 10 <sup>-1</sup>	4.5
4.0 × 10 <sup>7</sup>	1.299 × 10 <sup>-1</sup>	0.060 × 10 <sup>-1</sup>	4.6
6.0 × 10 <sup>7</sup>	1.113 × 10 <sup>-1</sup>	0.053 × 10 <sup>-1</sup>	4.7
8.0 × 10 <sup>7</sup>	1.001 × 10 <sup>-1</sup>	0.049 × 10 <sup>-1</sup>	4.9
1.0 × 10 <sup>8</sup>	9.280 × 10 <sup>-2</sup>	0.464 × 10 <sup>-2</sup>	5.0
1.5 × 10 <sup>8</sup>	8.307 × 10 <sup>-2</sup>	0.415 × 10 <sup>-2</sup>	5.0
2.0 × 10 <sup>8</sup>	7.810 × 10 <sup>-2</sup>	0.391 × 10 <sup>-2</sup>	5.0
4.0 × 10 <sup>8</sup>	6.647 × 10 <sup>-2</sup>	0.332 × 10 <sup>-2</sup>	5.0
6.0 × 10 <sup>8</sup>	5.746 × 10 <sup>-2</sup>	0.287 × 10 <sup>-2</sup>	5.0
8.0 × 10 <sup>8</sup>	4.979 × 10 <sup>-2</sup>	0.249 × 10 <sup>-2</sup>	5.0
1.0 × 10 <sup>9</sup>	4.321 × 10 <sup>-2</sup>	0.216 × 10 <sup>-2</sup>	5.0

<sup>a</sup>MeV/fission is a contraction of  $\frac{\text{MeV}\cdot\text{s}}{\text{fission}\cdot\text{s}}$

<sup>b</sup>Data for t greater than 10<sup>4</sup> are provided solely for use in Equations 3.45 and 3.46. They are not to be interpreted as standard decay heat values at these times.

Table 3-4  
 PROPOSED (ANS-5.1)  
 TABULAR DATA FOR STANDARD DECAY HEAT POWER FOR THERMAL FISSION OF Pu<sup>239</sup> AND FOR  
 IRRADIATION OF 10<sup>13</sup> SEC

Time After Shutdown, t(sec)	Decay Heat Power, D <sub>P3</sub> (t,∞) (MeV/fission) <sup>a</sup>	One Sigma Uncertainty, D <sub>P3</sub> (t,∞) (MeV/fission)	Percent Uncertainty
1.0×10 <sup>0</sup>	9.534×10 <sup>0</sup>	1.030×10 <sup>0</sup>	11.0
1.5×10 <sup>0</sup>	9.349×10 <sup>0</sup>	0.986×10 <sup>0</sup>	11.0
2.0×10 <sup>0</sup>	9.195×10 <sup>0</sup>	0.946×10 <sup>0</sup>	10.0
4.0×10 <sup>0</sup>	8.740×10 <sup>0</sup>	0.851×10 <sup>0</sup>	9.7
6.0×10 <sup>0</sup>	8.422×10 <sup>0</sup>	0.789×10 <sup>0</sup>	9.4
8.0×10 <sup>0</sup>	8.173×10 <sup>0</sup>	0.744×10 <sup>0</sup>	9.1
1.0×10 <sup>1</sup>	7.969×10 <sup>0</sup>	0.707×10 <sup>0</sup>	8.9
1.5×10 <sup>1</sup>	7.572×10 <sup>0</sup>	0.644×10 <sup>0</sup>	8.5
2.0×10 <sup>1</sup>	7.274×10 <sup>0</sup>	0.591×10 <sup>0</sup>	8.1
4.0×10 <sup>1</sup>	6.522×10 <sup>0</sup>	0.477×10 <sup>0</sup>	7.3
6.0×10 <sup>1</sup>	6.064×10 <sup>0</sup>	0.416×10 <sup>0</sup>	6.9
8.0×10 <sup>1</sup>	5.737×10 <sup>0</sup>	0.377×10 <sup>0</sup>	6.6
1.0×10 <sup>2</sup>	5.487×10 <sup>0</sup>	0.349×10 <sup>0</sup>	6.4
1.5×10 <sup>2</sup>	5.049×10 <sup>0</sup>	0.311×10 <sup>0</sup>	6.2
2.0×10 <sup>2</sup>	4.760×10 <sup>0</sup>	0.283×10 <sup>0</sup>	5.9
4.0×10 <sup>2</sup>	4.138×10 <sup>0</sup>	0.238×10 <sup>0</sup>	5.8
6.0×10 <sup>2</sup>	3.799×10 <sup>0</sup>	0.216×10 <sup>0</sup>	5.7
8.0×10 <sup>2</sup>	3.559×10 <sup>0</sup>	0.201×10 <sup>0</sup>	5.6
1.0×10 <sup>3</sup>	3.371×10 <sup>0</sup>	0.189×10 <sup>0</sup>	5.6
1.5×10 <sup>3</sup>	3.024×10 <sup>0</sup>	0.167×10 <sup>0</sup>	5.5
2.0×10 <sup>3</sup>	2.780×10 <sup>0</sup>	0.152×10 <sup>0</sup>	5.5
4.0×10 <sup>3</sup>	2.242×10 <sup>0</sup>	0.117×10 <sup>0</sup>	5.2
6.0×10 <sup>3</sup>	1.979×10 <sup>0</sup>	0.098×10 <sup>0</sup>	5.0
8.0×10 <sup>3</sup>	1.820×10 <sup>0</sup>	0.087×10 <sup>0</sup>	4.8
1.0×10 <sup>4</sup>	1.709×10 <sup>0</sup>	0.080×10 <sup>0</sup>	4.7
1.5×10 <sup>4b</sup>	1.533×10 <sup>0</sup>	0.069×10 <sup>0</sup>	4.5
2.0×10 <sup>4</sup>	1.425×10 <sup>0</sup>	0.062×10 <sup>0</sup>	4.4
4.0×10 <sup>4</sup>	1.196×10 <sup>0</sup>	0.050×10 <sup>0</sup>	4.2
6.0×10 <sup>4</sup>	1.076×10 <sup>0</sup>	0.044×10 <sup>0</sup>	4.1
8.0×10 <sup>4</sup>	9.972×10 <sup>-1</sup>	0.406×10 <sup>-1</sup>	4.1

Table 3-4 (Continued)  
 PROPOSED (ANS-5.1)  
 TABULAR DATA FOR STANDARD DECAY HEAT POWER FOR THERMAL FISSION OF Pu<sup>239</sup> AND FOR  
 IRRADIATION OF 10<sup>13</sup> SEC

Time After Shutdown, t(sec)	Decay Heat Power, D <sub>P3</sub> (t,∞) (MeV/fission) <sup>a</sup>	One Sigma Uncertainty, D <sub>P3</sub> (t,∞) (MeV/fission)	Percent Uncertainty
1.0 × 10 <sup>5</sup>	9.408 × 10 <sup>-1</sup>	0.378 × 10 <sup>-1</sup>	4.0
1.5 × 10 <sup>5</sup>	8.477 × 10 <sup>-1</sup>	0.336 × 10 <sup>-1</sup>	4.0
2.0 × 10 <sup>5</sup>	7.888 × 10 <sup>-1</sup>	0.309 × 10 <sup>-1</sup>	3.9
4.0 × 10 <sup>5</sup>	6.634 × 10 <sup>-1</sup>	0.258 × 10 <sup>-1</sup>	3.9
6.0 × 10 <sup>5</sup>	5.943 × 10 <sup>-1</sup>	0.231 × 10 <sup>-1</sup>	3.9
8.0 × 10 <sup>5</sup>	5.461 × 10 <sup>-1</sup>	0.213 × 10 <sup>-1</sup>	3.9
1.0 × 10 <sup>6</sup>	5.096 × 10 <sup>-1</sup>	0.199 × 10 <sup>-1</sup>	3.9
1.5 × 10 <sup>6</sup>	4.463 × 10 <sup>-1</sup>	0.176 × 10 <sup>-1</sup>	3.9
2.0 × 10 <sup>6</sup>	4.045 × 10 <sup>-1</sup>	0.160 × 10 <sup>-1</sup>	4.0
4.0 × 10 <sup>6</sup>	3.163 × 10 <sup>-1</sup>	0.128 × 10 <sup>-1</sup>	4.1
6.0 × 10 <sup>6</sup>	2.742 × 10 <sup>-1</sup>	0.114 × 10 <sup>-1</sup>	4.1
8.0 × 10 <sup>6</sup>	2.477 × 10 <sup>-1</sup>	0.105 × 10 <sup>-1</sup>	4.2
1.0 × 10 <sup>7</sup>	2.282 × 10 <sup>-1</sup>	0.099 × 10 <sup>-1</sup>	4.3
1.5 × 10 <sup>7</sup>	1.945 × 10 <sup>-1</sup>	0.085 × 10 <sup>-1</sup>	4.4
2.0 × 10 <sup>7</sup>	1.728 × 10 <sup>-1</sup>	0.076 × 10 <sup>-1</sup>	4.4
4.0 × 10 <sup>7</sup>	1.302 × 10 <sup>-1</sup>	0.059 × 10 <sup>-1</sup>	4.6
6.0 × 10 <sup>7</sup>	1.099 × 10 <sup>-1</sup>	0.052 × 10 <sup>-1</sup>	4.7
8.0 × 10 <sup>7</sup>	9.741 × 10 <sup>-2</sup>	0.473 × 10 <sup>-2</sup>	4.9
1.0 × 10 <sup>8</sup>	8.931 × 10 <sup>-2</sup>	0.447 × 10 <sup>-2</sup>	5.0
1.5 × 10 <sup>8</sup>	7.858 × 10 <sup>-2</sup>	0.393 × 10 <sup>-2</sup>	5.0
2.0 × 10 <sup>8</sup>	7.344 × 10 <sup>-2</sup>	0.367 × 10 <sup>-2</sup>	5.0
4.0 × 10 <sup>8</sup>	6.268 × 10 <sup>-2</sup>	0.313 × 10 <sup>-2</sup>	5.0
6.0 × 10 <sup>8</sup>	5.466 × 10 <sup>-2</sup>	0.273 × 10 <sup>-2</sup>	5.0
8.0 × 10 <sup>8</sup>	4.782 × 10 <sup>-2</sup>	0.239 × 10 <sup>-2</sup>	5.0
1.0 × 10 <sup>9</sup>	4.195 × 10 <sup>-2</sup>	0.210 × 10 <sup>-2</sup>	5.0

<sup>a</sup>MeV fission is a contraction of  $\frac{\text{MeV}\cdot\text{s}}{\text{fission}\cdot\text{s}}$

<sup>b</sup>Data for t greater than 10<sup>7</sup> are provided solely for use in Equations 3.45 and 3.46. They are not to be interpreted as standard decay heat values at these times.

Let  $N_U(t)$  be the atom density in atoms/b-cm of  $U^{239}$  at time  $t$  in seconds after the startup of the reactor. Likewise let  $N_N(t)$  be the atom density of  $Np^{239}$ . These quantities are determined by linear, first-order differential equations:

$$\frac{dN_U(t)}{dt} = \Sigma_{c8}\phi - (\lambda_U + \sigma_{aU}\phi) N_U \quad (3-1)$$

$$\frac{dN_N(t)}{dt} = \lambda_U N_U - (\lambda_N + \sigma_{aN}\phi) N_N \quad (3-2)$$

where  $\lambda_U$  and  $\lambda_N$  are the decay constants in  $\text{sec}^{-1}$  of  $U^{239}$  and  $Np^{239}$ ,  $\sigma_{aU}$  and  $\sigma_{aN}$  are the absorption cross sections in barns,  $\phi$  is the thermal flux in neutrons/cm<sup>2</sup> - sec and  $\Sigma_{c8}$  is the macroscopic capture cross section of  $U^{238}$ .

The initial conditions specify that the atom densities are zero at the time of startup:

$$N_U(0) = N_N(0) = 0 \quad (3-3)$$

It is conservatively assumed that the absorption cross sections of both isotopes are zero. This maximizes the concentrations at the time of shutdown. Multiplying the first equation by  $e^{\lambda_U t}$  and rearranging:

$$\frac{d}{dt} (e^{\lambda_U t} N_U(t)) = \Sigma_{c8} \phi e^{\lambda_U t} \quad (3-4)$$

Similarly:

$$\frac{d}{dt} (e^{\lambda_N t} N_N(t)) = \lambda_U N_U e^{\lambda_N t} \quad (3-5)$$

The solutions of these equations consist of a general solution to the homogeneous equation and a particular solution to the inhomogeneous equation:

$$N_U(t) = N_U(0)e^{-\lambda_U t} - \Sigma_{c8}\phi \int_0^t dt' e^{\lambda_U(t-t')} \quad (3-6)$$

$$N_N(t) = N_N(0)e^{-\lambda_N t} - \lambda_U \int_0^t dt' N_U(t') e^{\lambda_N(t-t')} \quad (3-7)$$

Let  $t=T$  be the reactor operating time. Then employing the initial conditions and performing the integrations:

$$N_U(T) = \frac{\Sigma_{c8}\phi}{\lambda_U} \left\{ 1 - e^{-\lambda_U T} \right\} \quad (3-8)$$

$$N_N(T) = \frac{\Sigma_{c8}\phi}{\lambda_N} \left\{ 1 - \frac{\lambda_U}{\lambda_U - \lambda_N} e^{-\lambda_N T} + \frac{\lambda_N}{\lambda_U - \lambda_N} e^{-\lambda_U T} \right\} \quad (3-9)$$

Now let  $t$  be the time after shutdown. The differential equations governing the densities are obtained from the previous set by simply setting the flux equal to zero:

$$\frac{dN_U(t)}{dt} = -\lambda_U N_U \quad (3-10)$$

$$\frac{dN_N(t)}{dt} = \lambda_U N_U - \lambda_N N_N \quad (3-11)$$

The initial conditions are simply the values of the densities at the time of shutdown. Transforming the equations as before:

$$\frac{d}{dt}(e^{\lambda_U t} N_U(t)) = 0 \quad (3-12)$$

$$\frac{d}{dt}(e^{\lambda_N t} N_N(t)) = \lambda_U N_U e^{\lambda_N t} \quad (3-13)$$

The solutions of these equations are:

$$N_U(t) = N_U(0) e^{-\lambda_U t} \quad (3-14)$$

$$\begin{aligned} N_N(t) &= N_N(0) e^{-\lambda_N t} - \lambda_U N_U(0) \int_0^t dt' e^{i\lambda_N t' - \lambda_U t' - \lambda_N t'} \\ &= N_N(0) e^{-\lambda_N t} - \frac{\lambda_U N_U(0)}{\lambda_U - \lambda_N} \left\{ e^{-\lambda_N t} - e^{-\lambda_U t} \right\} \end{aligned} \quad (3-15)$$

Substituting the expressions for the initial values:

$$N_U(t) = \frac{\Sigma_{ca}\phi}{\lambda_U} \left[ 1 - e^{-\lambda_U T} \right] e^{-\lambda_U t} \quad (3-16)$$

$$\begin{aligned} N_N(t) &= \frac{\Sigma_{ca}\phi}{\lambda_N} \left\{ \left[ 1 - \frac{\lambda_U}{\lambda_U - \lambda_N} e^{-\lambda_N T} - \frac{\lambda_N}{\lambda_U - \lambda_N} e^{-\lambda_U T} \right] e^{-\lambda_N t} \right. \\ &\quad \left. + \frac{\lambda_N}{\lambda_U - \lambda_N} \left[ 1 - e^{-\lambda_U T} \right] \left[ e^{-\lambda_N t} - e^{-\lambda_U t} \right] \right\} \\ &= \frac{\Sigma_{ca}\phi}{\lambda_N} \left\{ \frac{\lambda_U}{\lambda_U - \lambda_N} \left[ 1 - e^{-\lambda_N T} \right] e^{-\lambda_N t} \right. \\ &\quad \left. - \frac{\lambda_N}{\lambda_U - \lambda_N} \left[ 1 - e^{-\lambda_U T} \right] e^{-\lambda_U t} \right\} \end{aligned} \quad (3-17)$$

The total power released by the actinides as a function of the time t after shutdown can now be easily computed. Let this quantity be  $D_A(t, T)$  where T is the irradiation time or equivalently the reactor operating time. The decay rates of the actinides are equal to  $\lambda_U N_U(t)$  and  $\lambda_N N_N(t)$ . Multiplying these quantities by their respective sensible energy release per decay (from Table 2-17) and then dividing by the fission rate in the reactor prior to shutdown, results in the energy release per fission:

$$D_A(t, T) = \frac{Q_U \lambda_U N_U(t) + Q_N \lambda_N N_N(t)}{\Sigma_f \phi} \quad (3-18)$$

where  $\Sigma_f$  is the fission cross section. It is very convenient to write this result in terms of a parameter C which is only a function of the reactor):

$$C = \frac{\Sigma_{ca}}{\Sigma_f} \quad (3-19)$$

and a function  $A(t,T)$  which only depends on the physical properties of the actinides:

$$\begin{aligned}
 A(t,T) = & Q_U \left[ 1 - e^{-\lambda_U T} \right] e^{-\lambda_U t} \\
 & + Q_N \left\{ \frac{\lambda_U}{\lambda_U - \lambda_N} \left[ 1 - e^{-\lambda_N T} \right] e^{-\lambda_N t} \right. \\
 & \left. - \frac{\lambda_N}{\lambda_U - \lambda_N} \left[ 1 - e^{-\lambda_U T} \right] e^{-\lambda_U t} \right\}
 \end{aligned} \tag{3-20}$$

Then

$$D_A(t,T) = C \cdot A(t,T) \tag{3-21}$$

Note that in the case of an infinite irradiation time  $T = \infty$ ,  $A(t,T)$  reduces to:

$$\begin{aligned}
 A(t,\infty) = & Q_U e^{-\lambda_U t} + Q_N \left\{ \frac{\lambda_U}{\lambda_U - \lambda_N} e^{-\lambda_N t} \right. \\
 & \left. - \frac{\lambda_N}{\lambda_U - \lambda_N} e^{-\lambda_U t} \right\}
 \end{aligned} \tag{3-22}$$

### 3.1.3 Delayed Neutron Induced Fission Heat

When a reactor shuts down either during normal or accident conditions, the power level does not drop immediately to zero. Instead it decays away with time due to fissions caused by delayed neutrons. The decay rate is determined by the physical properties of the reactor fuel and by the magnitude of the negative reactivity insertion. During a LOCA there are two main sources of negative reactivity: void feedback which begins immediately and control rod insertion which is delayed for a short period due to instrument response and the inertia of the control rods.

The current method for determining the decay of the fission heat is a computer code SCARED. SCARED is based on a one-dimensional coupled nuclear and thermal-hydraulic model. It uses a single neutron energy group and makes the prompt jump approximation. The thermal-hydraulic model is identical to the model in the SCAT code. Further details about the SCARED model and its application may be found in pages I-10 to I-35 of *General Electric Company Analytical Model for Loss-of-Coolant Analysis in Accordance with 10 CFR 50, Appendix K*. On the basis of a number of SCARED analyses, it was concluded that the fission rate decay of a BWR/6 reactor was the most conservative. Physically, this is due to a slower blowdown rate which induces a smaller void feedback reactivity than for other plants. The BWR/6 results are presented in tabular form in Table 3-5.

An independent review has concluded that the current model is likely to be overconservative by approximately 10° to 40°F in peak cladding temperature. This is due in part to recent improvements in the methods for computing void feedback and in part to the fact that a single curve is used to represent all plants, small as well as large. However, until such time as a more advanced theoretical model becomes available, it is recommended that Table 3-5 be used for all ECCS analyses.

### 3.1.4 Decay Heat from Structural Materials

Decay heat produced by neutron activation of structural materials is a potential source of heat during a LOCA. However, it will be shown in this subsection that such heat sources are extremely small and may be safely neglected.

The principal structural material in a BWR core is zirconium. (Stainless steel is present in the control rods, but the control rods are normally only partially inserted and in addition are subject to low neutron flux levels.) Table 3-6 lists the stable isotopes of zirconium and gives their fractional abundance, thermal cross section, and resonance integrals<sup>12</sup>. In the far right hand column is the decay energy of the activated products of a neutron capture event in the indicated isotope. These decay energies are consistent with Table 2-13 and do not include the energy of antineutrinos. The total decay power is related to the relative capture rate  $r_i$ , among the individual isotopes.  $r_i$  may be computed as follows:

$$r_i = f_i \left[ \sigma_i \phi_{th} - R_i \frac{\phi_{res}}{\ln(E_{res}/E_{th})} \right] \quad (3-23)$$

where  $f_i$  is the fractional abundance of isotope  $i$ ,  $\sigma_i$  is the thermal cross section,  $r_i$  is the resonance integral,  $\phi_{th}$  is the thermal flux,  $\phi_{res}$  is the resonance flux, and  $E_{res}$  and  $E_{th}$  are the upper limits of the resonance and thermal groups, respectively. The decay heat power  $P_{2r}$  at the time of shutdown may be computed as follows:

$$P_{2r} = R \frac{\sum_{i=1}^5 Q_i r_i}{\sum_{i=1}^5 r_i} \quad (3-24)$$

where  $R$  is the ratio of captures in zirconium to fissions in the reactor prior to shutdown, and  $Q_i$  is the decay energy for isotope  $i$ .

Representative values for the reactor-dependent quantities were obtained from the reload bundle 80250 at 40% voids and 10 GWd/t:

$$\begin{aligned} \frac{\phi_{res}}{\phi_{th}} &= 1.4721 \\ E_{th} &= 0.683 \text{ eV} \\ E_{res} &= 5.53 \times 10^3 \text{ eV} \\ R &= 0.0483 \end{aligned} \quad (3-25)$$

Using these values and the constants from Table 3-6 results in a decay power of:

$$P_{2r} = 0.013 \text{ MeV} \cdot \text{fission} \quad (3-26)$$

This is almost three orders of magnitude less than the decay heat from fission products and may therefore be neglected.

Table 3.5  
RELATIVE FISSION RATE AFTER LOCA

Time After Shutdown, t(sec)	Relative Fission Rate, F(t)
0.0	1.000
0.1	0.982
0.2	0.920
0.4	0.724
0.6	0.559
0.8	0.457
1.0	0.293
2.0	0.101
3.0	$0.378 \times 10^{-1}$
4.0	$0.191 \times 10^{-1}$
5.0	$0.109 \times 10^{-1}$
6.0	$0.834 \times 10^{-2}$
7.0	$0.744 \times 10^{-2}$
8.0	$0.600 \times 10^{-2}$
9.0	$0.460 \times 10^{-2}$
10.0	$0.330 \times 10^{-2}$
20.0	$0.130 \times 10^{-2}$
30.0	$0.900 \times 10^{-3}$
40.0	$0.500 \times 10^{-3}$
50.0	$0.400 \times 10^{-3}$
60.0	$0.290 \times 10^{-3}$

Table 3.6  
PROPERTIES OF ZIRCONIUM ISOTOPES

Atomic Number	Fractional Abundance, $f_i$	Thermal Cross Section, $\sigma_i$	Resonance Integral, $R_i$	Decay Energy, Q.(MeV)
90	0.514	0.03	0.2	0.0
91	0.112	1.1	5.	0.0
92	0.171	0.2	0.6	0.0
94	0.175	0.055	0.3	1.65
96	0.028	0.02	5.	2.64

### 3.2 SPECIFICATIONS FOR DECAY HEAT MODELS

The energy sources described in the previous subsection must be combined together to form a decay heat curve for use in ECCS calculations. This is a relatively straightforward process. Nevertheless, three distinct decay heat models must be presented. The first will be the model currently in use. The second model will be an improved version of the current model with greater technical accuracy and justification, but still based upon the current ANS-5 decay heat standard<sup>2,3</sup>. The third and final model will be based on the revised standard proposed by the ANS-5.1 working group<sup>4</sup>.

The most convenient way of expressing a decay heat curve is in terms of power relative to the power prior to shutdown:

$$R(t) = \frac{P(t)}{P(o)} \quad (3-27)$$

where  $t$  is the time after shutdown.

The numerator is determined by multiplying the decay heat power,  $D(t)$ , (measured in MeV/fission) by the fission rate in the reactor:

$$P(t) = D(t) \Sigma_f \phi \quad (3-28)$$

The initial power is also proportional to the fission rate:

$$P(o) = \bar{Q} \Sigma_f \phi \quad (3-29)$$

where  $\bar{Q}$  is the average energy release per fission. Then

$$R(t) = \frac{D(t)}{\bar{Q}} \quad (3-30)$$

since the fission rate cancels out,  $D(t)$  is simply the sum of the energy sources mentioned in the previous section:

$$R(t) = \frac{U \cdot D_s(t, \infty) + C \cdot A(t, \infty) + a \cdot F(t)}{\bar{Q}} \quad (3-31)$$

where, as before,  $D_s(t, \infty)$  is the current ANS-5 decay heat energy per fission for an infinite reactor operating time (Table 3-1),  $A(t, \infty)$  is the actinide contribution (Equation 3-22) and  $F(t)$  is the relative fission rate (Table 3-5). The constant  $U$  is a conservative factor intended to ensure that the decay heat is not underestimated due to a bias in the decay heat experiments. The value of this constant is currently fixed by 10CFR50 Appendix K' at the value of 1.2.  $C$  is the actinide normalization constant as before and " $a$ " is a constant which is necessary to ensure that the initial relative power,  $R(o)$ , is equal to one. In other words, the contribution from direct fission sources is found by subtracting out the decay heat sources at time zero:

$$R(t) = \frac{1}{\bar{Q}} \left\{ U \cdot D_s(t, \infty) + C \cdot A(t, \infty) - \left[ \bar{Q} - U \cdot D_s(o, \infty) - C \cdot A(o, \infty) \right] F(t) \right\} \quad (3-32)$$

For the purpose of understanding the current decay heat model, Model 1, which will be denoted by  $R_1(t)$ , it is necessary to generalize this model as follows:

$$R_1(t) = \frac{U \cdot D_s(t, \infty)}{\bar{Q}'} + \frac{C \cdot A(t, \infty)}{\bar{Q}''} - \left( 1 - \frac{U \cdot D_s(o, \infty)}{\bar{Q}'} - \frac{C \cdot A(o, \infty)}{\bar{Q}''} \right) F(t) \quad (3-33)$$

where  $\bar{Q}'$  and  $\bar{Q}''$  are separate constants for the normalization of the fission product and actinide contributions. The current value of  $\bar{Q}''$  is 207.3 MeV/fission, which was chosen to be representative of an equilibrium cycle. Originally, it was intended that this value be used for  $\bar{Q}'$  also. However, the ANS-5 standard<sup>3</sup> requires that a value different from the nominal and conservative value of 200 MeV/fission be adequately justified. The Nuclear Regulatory Commission has concluded that the higher value was *not*, in fact, adequately justified and therefore the value  $\bar{Q}' = 200$  MeV/fission is currently used. Also used in the current decay heat model is the value of 0.68 for the actinide normalization constant. The values for the sensible energy releases for the decay of the actinides are as presented as the "current values" in Table 2-17.

The second decay heat model is intended to resolve the problems associated with the energy per fission values and to improve the technical validity of the calculations. To this end, the reactor-dependent quantities  $\bar{Q}$  and C are now evaluated as functions of exposure. The relative power for this model,  $R_{II}(t, E)$ , is evaluated as follows:

$$R_{II}(t, E) = \frac{1}{\bar{Q}(E)} \left[ U \cdot D_s(t, \infty) + C(E) \cdot A(t, \infty) - \left( \bar{Q}(E) - U \cdot D_s(0, \infty) - C(E) \cdot A(0, \infty) \right) F(t) \right] \quad (3-34)$$

The actinide decay energies for this model are the "recommended" values given in Table 2-17. It is assumed in this model as in Model I, that the *actinide* contribution is computed on the basis of an infinite irradiation period. This is not a direct requirement of 10CFR50 Appendix K<sup>1</sup>. However, the difference is very small since the actinides saturate very rapidly (within a few days). Therefore, it is convenient and conservative as well to assume an infinite irradiation period.

The average energy per fission is calculated by weighting the energy release for each isotope,  $Q_i$ , by its fractional contribution  $f_i(E)$  to total fissions:

$$\bar{Q}(E) = \sum_{i=1}^3 Q_i f_i(E) \quad (3-35)$$

where 
$$\sum_{i=1}^3 f_i(E) = 1.$$

The summation is carried out only for the principal isotopes:  $U^{235}$  ( $i=1$ ),  $U^{238}$  ( $i=2$ ) and  $Pu^{239}$  ( $i=3$ ). The value of  $Q_i$  for each isotope is taken to be its recommended value from Table 2-11. Fissions in  $Pu^{241}$  are included with those of  $Pu^{239}$  because of the strong similarity between the two isotopes. This is a conservative assumption since the energy per fission for  $Pu^{241}$  is higher than for  $Pu^{239}$ . This causes the decay heat to be slightly higher when  $Pu^{241}$  is lumped with  $Pu^{239}$  than when they are considered separately. Fissions in all other isotopes beyond the four already mentioned are included with  $U^{235}$ . Ordinarily these fissions account for only a fraction of 1% of the total fissions. As a direct result of this latter assumption the fission fraction  $f_1(E)$  can always be computed as follows:

$$f_1(E) = 1 - f_2(E) - f_3(E) \quad (3-36)$$

Equations 3-34, 3-35, and 3-36 constitute decay heat Model II. This model requires knowledge of three functions,  $C(E)$ ,  $f_2(E)$ , and  $f_3(E)$ , which depend on exposure and on the reactor fuel itself. In order to determine the sensitivity of the model to these functions, a large number of decay heat calculations have been performed for different fuel bundles at various exposures and void fractions. The results of these calculations are presented in Table 3-7. Bundle 8D250 is a very common reload bundle. It is an 8x8 D lattice with an average enrichment of 2.50%. BF1T2 is Browns' Ferry 1 Type 2 initial fuel. This is a 7x7 lattice. Bundle 8D274 has the highest enrichment of the standard reload bundles. Similarly, 8DR303 is the highest enrichment available for retrofit fuel. B6-183 is a BWR/6 bundle with the lowest enrichment available except for the natural uranium fuel. These bundles clearly represent a broad spectrum of the type of fuel used in BWR's.

**Table 3-7**  
**DECAY HEAT COMPARISON FOR DIFFERENT BUNDLES AT VARIOUS EXPOSURES AND VOIDS**  
**E(GWd/t) = 0**

Bundle:	8D250	BF1T2	8D274	8DR303	B6-183
Voids %	40	40	40	40	40
C(E)	0.62340	0.62932	0.61435	0.57501	0.68802
f <sub>1</sub> (E)	0.92527	0.92372	0.92323	0.92902	0.92671
f <sub>2</sub> (E)	0.07473	0.07628	0.07677	0.07098	0.07329
f <sub>3</sub> (E)	0.0	0.0	0.0	0.0	0.0
Q(E)	202.07	202.07	202.08	202.06	202.06
R <sub>1</sub> (t)					
t = 1 sec	0.3463				
t = 100 sec	0.04257				
R <sub>11</sub> (t,E)					
t = 1 sec	0.3457	0.3457	0.3456	0.3455	0.3459
t = 100 sec	0.04197	0.04199	0.04193	0.04176	0.04224
R <sub>111</sub> (t,T,E) <sup>a</sup>					
t = 1 sec	0.3404	0.3404	0.3404	0.3402	0.3406
t = 100 sec	0.03548	0.03551	0.03544	0.03528	0.03576

<sup>a</sup>u = 1.07

**DECAY HEAT COMPARISON FOR DIFFERENT BUNDLES AT VARIOUS EXPOSURES AND VOIDS**  
**E(GWd/t) = 10**

Bundle:	8D250	8D250	8D250	BF1T2	8D274	8DR303	B6-183
Voids %	40	0	70	40	40	40	40
C(E)	0.65076	0.58805	0.71518	0.65790	0.63906	0.59910	0.71881
f <sub>1</sub> (E)	0.56171	0.60159	0.52257	0.55481	0.58138	0.61753	0.47541
f <sub>2</sub> (E)	0.07940	0.06387	0.10069	0.08106	0.08125	0.07481	0.07891
f <sub>3</sub> (E)	0.35889	0.33454	0.37674	0.36413	0.33737	0.30766	0.44568
Q(E)	205.14	204.87	205.36	205.19	204.96	204.68	205.87
R(t)							
t = 1 sec	0.3463						
t = 100 sec	0.04257						
R <sub>1</sub> (t,E)							
t = 1 sec	0.3450	0.3448	0.3451	0.3450	0.3450	0.3449	0.3450
t = 100 sec	0.04145	0.04124	0.04168	0.04147	0.04144	0.04133	0.04159
R <sub>11</sub> (t,T,E)							
t = 1 sec	0.3363	0.3363	0.3364	0.3363	0.3365	0.3367	0.3355
t = 100 sec	0.03373	0.03360	0.03390	0.03374	0.03379	0.03378	0.03358

Table 3-7 (continued)

DECAY HEAT COMPARISON FOR DIFFERENT BUNDLES AT VARIOUS EXPOSURES AND VOIDS  
E(GWd/t) = 20

Bundle:	8D250	BF1T2	8D274	8DR303	B6-183
Voids %	40	40	40	40	40
C(E)	0.70446	0.71296	0.68106	0.63842	0.81568
f <sub>1</sub> (E)	0.37846	0.37178	0.40579	0.45024	0.26769
f <sub>2</sub> (E)	0.08267	0.08481	0.08344	0.07673	0.08864
f <sub>3</sub> (E)	0.53887	0.54341	0.51077	0.47303	0.64367
Q(E)	206.68	206.72	206.44	206.10	207.59
R <sub>i</sub> (t)					
t = 1 sec	0.3463				
t = 100 sec	0.04257				
R <sub>ii</sub> (t,E)					
t = 1 sec	0.3447	0.3448	0.3447	0.3447	0.3448
t = 100 sec	0.04137	0.04139	0.04132	0.04121	0.04165
R <sub>iii</sub> (t,T,E)					
t = 1 sec	0.3344	0.3344	0.3347	0.3349	0.3336
t = 100 sec	0.03304	0.03306	0.03309	0.03310	0.03298

DECAY HEAT COMPARISON FOR DIFFERENT BUNDLES AT VARIOUS EXPOSURES AND VOIDS  
E(GWd/t) = 30

Bundle:	8D250	BF1T2	8D274	8DR303	B6-183
Voids %	40	40	40	40	40
C(E)	0.79789	0.80120	0.76561	0.71588	0.89320
f <sub>1</sub> (E)	0.23333	0.22961	0.26741	0.31588	0.13193
f <sub>2</sub> (E)	0.09253	0.09445	0.09257	0.08333	0.09729
f <sub>3</sub> (E)	0.67414	0.67594	0.64002	0.60079	0.77078
Q(E)	207.86	207.89	207.57	207.21	208.70
R <sub>i</sub> (t)					
t = 1 sec	0.3463				
t = 100 sec	0.04257				
R <sub>ii</sub> (t,E)					
t = 1 sec	0.3447	0.3447	0.3447	0.3446	0.3448
t = 100 sec	0.04152	0.04153	0.04144	0.04131	0.04174
R <sub>iii</sub> (t,T,E)					
t = 1 sec	0.3332	0.3332	0.3335	0.3337	0.3324
t = 100 sec	0.03275	0.03275	0.03278	0.03278	0.03266

**Table 3-7 (continued)**  
**DECAY HEAT COMPARISON FOR DIFFERENT BUNDLES AT VARIOUS EXPOSURES AND VOIDS**  
**E(GWd/t) = 40**

<b>Bundle:</b>	<b>8D250</b>	<b>BF1T2</b>	<b>8D274</b>	<b>8DR303</b>	<b>B6-183</b>
Voids %	40	40	40	40	40
C(E)	0.86862	0.86483	0.83920	0.80174	0.93477
f <sub>1</sub> (E)	0.12820	0.12726	0.15855	0.19630	0.06017
f <sub>2</sub> (E)	0.10001	0.10178	0.10049	0.09172	0.10229
f <sub>3</sub> (E)	0.77179	0.77096	0.74096	0.71198	0.83754
Q(E)	208.72	208.72	208.46	208.18	209.29
R <sub>i</sub> (t)					
t = 1 sec	0.3463				
t = 100 sec	0.04257				
R <sub>ii</sub> (t,E)					
t = 1 sec	0.3447	0.3447	0.3447	0.3447	0.3448
t = 100 sec	0.04164	0.04162	0.04157	0.04147	0.04180
R <sub>iii</sub> (t,T,E)					
t = 1 sec	0.3324	0.3324	0.3326	0.3328	0.3318
t = 100 sec	0.03255	0.03254	0.03258	0.03257	0.03249

Below the bundle identification in Table 3-7 are the exposure and void fraction followed by  $C(E)$ ,  $f_2(E)$  and  $f_3(E)$  as evaluated by the official GE lattice analysis program. Below this is the value of  $Q(E)$  as determined by Equation 3-35. Values of the decay heat at the indicated times are given for the three decay heat models. The third model will be discussed later. Decay heat Model I, the current model is independent of the bundle type and exposure. Model II, the improved model, does have a dependency on exposure. This dependency is very slight at  $t=1$  second because the direct fission power still dominates. At  $t=100$  seconds the fission power is no longer present and the decay heat is simply the sum of the fission product and actinide contributions. The dependency on exposure is therefore longer at this time. The variation of Model II with voids is illustrated by the calculations on 8D250 at 10 GWd/t. The decay heat is shown to vary by no more than 0.5% from the nominal value at 40% voids. What is even more remarkable is that the decay heat for all bundle types at 10 GWd/t and 40% voids also varies by less than 0.5% from the nominal value of 8D250 at 40% voids. This is the result of a cancellation of effects with respect to the fission product and actinide contributions. The higher the enrichment of the bundle, the lower the value will be of energy release per fission. This implies a higher fission rate and hence a higher contribution from fission products. On the other hand, the higher the enrichment of the bundle, the smaller the value will be of  $C(E)$ . This causes the actinide contribution to fall. These two effects cancel each other and the result is a decay heat value which is nearly independent of bundle type. At exposures higher than 10 GWd/t, the variation among the bundles increases somewhat, but in all cases is less than 1%.

As a direct result of these comparisons, the nominal values of the functions  $C(E)$ ,  $f_2(E)$  and  $f_3(E)$  were chosen as corresponding to the values for bundle 8D250 at 40% voids. This is justifiable because the resulting decay heat values fall in between the other values and thus represent an average for all bundles. In any case, the deviation from these nominal values is very slight.

In order to make the implementation of Model II easier and more reliable, fits for the three required functions  $C(E)$ ,  $f_2(E)$  and  $f_3(E)$  were generated. The actinide normalization constant,  $C(E)$ , was fit with a quadratic polynomial in exposure:

$$C(E) \equiv C_0 + C_1 E + C_2 E^2 \quad 0 \leq E \leq 40 \text{ GWd/t} \quad (3-37)$$

The values of the fit coefficient were determined by a least squares method based on seven exposure points:

$$\begin{aligned} C_0 &= 6.17298 \times 10^{-1} \\ C_1 &= 2.85865 \times 10^{-3} \\ C_2 &= 9.22303 \times 10^{-5} \end{aligned} \quad (3-38)$$

The largest error observed in the fitting process was  $-1.5\%$  and the root-mean-squared (rms) error was  $1.0\%$ . The fission fraction of  $U^{238}$  was also fit with a quadratic polynomial:

$$f_2(E) \equiv a_0 + a_1 E + a_2 E^2 \quad 0 \leq E \leq 40 \text{ GWd/t} \quad (3-39)$$

where

$$\begin{aligned} a_0 &= 7.52541 \times 10^{-2} \\ a_1 &= 2.57466 \times 10^{-4} \\ a_2 &= 9.51169 \times 10^{-6} \end{aligned} \quad (3-40)$$

The largest error in this fit was  $-1.9\%$  and the rms error was  $1.0\%$ . The fission fraction of  $Pu^{239}$  plus  $Pu^{241}$  was fit with a rational polynomial:

$$f_3(E) \equiv \frac{b_1 E + b_2 E^2 + b_3 E^3}{d_0 + d_1 E} \quad 0 \leq E \leq 40 \text{ GWd/t} \quad (3-41)$$

where

$$\begin{aligned} b_1 &= 1.00000 \\ b_2 &= 4.38985 \times 10^{-2} \end{aligned}$$

$$\begin{aligned}
 b_3 &= -3.34992 \times 10^{-4} \\
 d_0 &= 14.1680 \\
 d_1 &= 2.51999
 \end{aligned}
 \tag{3-42}$$

The largest error observed in this fit was +0.7% and the rms error was 0.3%.

In order to test the accuracy of these fits, decay heat calculations were made with Model II (and Model III to be described below) using both exact values for the three functions and the fits, Equations 3-37 through 3-42. The results are shown in Table 3-8. In all cases, the fits produce decay heat values which are correct to within 0.1%. This is certainly accurate enough to justify their use.

The principal feature of the third decay heat model, namely Model III, is the use of the proposed revised ANS standard decay heat curves<sup>4</sup>. A secondary feature of the new model is the ability to account for finite reactor operating times. The relative power,  $R_{III}(t, T, E)$ , at time  $t$  seconds after shutdown based on an operating time of  $T$  seconds is given by the following expression:

$$R_{III}(t, T, E) = \frac{1}{\bar{Q}(E)} \left[ U \cdot D_p(t, T) - C(E) \cdot A(t, T) - \left( \bar{Q}(E) - U \cdot D_p(0, T) - C(E) \cdot A(0, T) \right) F(t) \right]
 \tag{3-43}$$

The decay heat from fission products  $D_p(t, T)$  is evaluated by summing the contributions of  $U^{235}$ ,  $U^{238}$ , and  $Pu^{239}$  weighted by their respective fission fractions:

$$D_p(t, T) = \sum_{i=1}^3 f_i(E) D_{p_i}(t, T)
 \tag{3-44}$$

The decay heat for each isotope for a *finite* irradiation period is related to the decay heat for an *infinite* irradiation period in the following way:

$$D_{p_i}(t, T) = D_{p_i}(t, \infty) - D_{p_i}(t-T, \infty)
 \tag{3-45}$$

Therefore, the standard specifies only values for  $D_{p_i}(t, \infty)$ . These were presented in Tables 3-2, 3-3, and 3-4 of Sub-section 3.1.1. Combining the last two equations:

$$D_p(t, T) = \sum_{i=1}^3 f_i(E) [D_{p_i}(t, \infty) - D_{p_i}(t-T, \infty)]
 \tag{3-46}$$

**Table 3-8**  
**DECAY HEAT AT T=100 SEC FOR BUNDLE 8D250—**  
**COMPARISON BETWEEN EXACT CONSTANTS AND USE OF FITS**

E(Gwd/t):		0	10	20	30	40
$R_I(100)$		0.04257	—	—	—	—
$R_{II}(100, E)$	Exact	0.04197	0.04145	0.04137	0.04152	0.04164
	Fits	0.04194	0.04147	0.04139	0.04147	0.04168
$R_{III}(100, \infty, E)$	Exact	0.03548	0.03373	0.03304	0.03275	0.03255
	Fits	0.03545	0.03376	0.03307	0.03270	0.03259

The proposed standard specifies uncertainties as a function of time for each of three decay heat tables (see Tables 3-2, 3-3, and 3-4). It is therefore feasible to account for uncertainties in the data by adding  $2\sigma$  as a function of time to the tabular values. Instead, a simpler procedure is used here which utilizes a single time-independent factor  $U$  as in Models I and II. The value of  $U$  was chosen as the  $2\sigma$  uncertainty for 8D250 at 10 GWd:t and a time of 100 seconds after shutdown. This was computed to be 1.07.

The actinide contribution  $A(t, T)$  is now determined by Equation 3-20 rather than Equation 3-22. In cases where the irradiation time is unknown, it may be related directly to the exposure as follows:

$$T = \frac{\rho E}{\epsilon p}$$

where  $\rho$  is the smeared fuel density in gm/cc,  $p$  is the power density in watts/cc, and  $\epsilon$  is a conversion factor equal to  $1.04998 \times 10^{-6}$ .

At the present time, 10CFR50 Appendix K requires an infinite irradiation time. Therefore, all of the calculations which have so far been made on Model III were made with that assumption. These calculations have already been shown in Tables 3-7 and 3-8. In general, the decay heat values are 15% to 20% less than either Model I or Model II. This is a strong indication of the over-conservatism of the current ANS standard.

## 4. NUCLEAR ENERGY TRANSPORT AND DEPOSITION

The significant factor in loss-of-coolant (LOCA) analyses is not the origin of the energy being released but rather the location at which the energy is deposited. It is the local deposition of energy which causes the fuel rods and cladding to heat up. The principal method for energy transfer from one location to another is through gamma ray transport. It was pointed out in Section 2 that roughly one half of all the energy produced during a LOCA is in the form of gammas (see Table 2-12). It is therefore imperative that gamma transport effects be accounted for. It is also very advantageous since gamma transport always acts to flatten the peak energy deposition and therefore leads to reduced peak cladding temperatures.

Under normal power conditions gamma transport effects are far less substantial since the fraction of the energy released as gammas is much smaller (see Table 2-12). On the other hand, neutron energy transport becomes important under normal power conditions. Neutrons born in the fuel as a result of fission are likely to escape into the coolant and deposit their kinetic energy there in a series of "slowing down" interactions. This effect is at least as important as gamma transport under normal power conditions.

Gamma and neutron energy transport calculations and models will be presented in Subsection 4.1. In Subsection 4.2, the specifications for incorporating these models in ECCS calculations will be given.

### 4.1 EVALUATION OF ENERGY TRANSPORT MODELS

Energy transport is conveniently divided into three separate effects. These effects may be accounted for individually or all at once. It is, however, most convenient to consider each separately and then to combine them later. The first effect to be considered is the deposition of energy in structural materials. This is discussed in Subsection 4.1.1. The results of photon Monte Carlo calculations using the engineering computer program KRIS01 are presented in order to quantify the effect. The second major effect is the rod-to-rod gamma energy transport which flattens the relative rod power distribution. This is discussed in Subsection 4.1.2. The third effect to be considered is the transport of energy from bundle to bundle. This is presented in Subsection 4.1.3.

Two transport effects which are not considered in this report are axial gamma energy transport and radial gamma energy transport *within* fuel pellets. The former effect is potentially significant but methods to evaluate it accurately are not currently available at a reasonable cost and in any event it is certainly conservative to neglect it. The latter effect is very small and can also be neglected.

#### 4.1.1 Gamma and Neutron Energy Deposition

Current ECCS calculations are based upon  $S_0$  gamma transport calculations. Recently, a more powerful and more accurate method for performing gamma transport calculations has become available through the introduction of the computer program KRIS01. KRIS01 is a Monte Carlo program which may be used to solve transport problems involving photons, electrons, and positrons. The geometric representation of the problem is very general and allows the cylindrical material regions of the cladding and fuel pellets to be handled explicitly and precisely. The space, energy, and angular phase space is essentially continuous; however, the source distribution is limited to a small number of energy groups. The isotopic-dependent capture and fission rates for each fuel rod are used in combination with gamma spectra for capture and fission events in each isotope to produce a rod and energy group dependent gamma source distribution for input to KRIS01. For LOCA analyses this gamma source is restricted to delayed gammas and explicitly excludes prompt and capture gammas.

Gamma transport calculations using KRIS01 have been performed on two different bundles: 8D250, a common 8x8 reload bundle, and Brown's Ferry 1 Type 2 (BF1T2) an initial core 7x7 fuel. Descriptions of both bundles are given in Table 4-1. Each bundle was analyzed under both normal and LOCA conditions. The normal power calculations were performed with the control blade out. The LOCA transport calculations were performed with the blade in while the gamma source distribution for the LOCA case was computed with the blade out. This corresponds to

the most likely situation; namely, that the highest power node is uncontrolled before the LOCA but is controlled soon after the LOCA begins.

The fractional gamma energy depositions for each of the structural media of bundle 8D250 are shown in Table 4-2. The results of Scatena and Upham<sup>3</sup> are given first followed by the latest KRISO1 calculations, which employed 80 batches of 1000 source photons each. Results for both normal and LOCA conditions are shown. In general, the gamma energy deposition is closely related to the mass of the material. Since the fuel is the most massive component by far, most of the energy is deposited there. Of particular interest is the energy which is deposited outside of the fuel and cladding. This energy does not contribute to heating of the cladding and consequently to the peak cladding temperature.

As a rule, the agreement between the previous results and KRISO1 results is reasonably close. The KRISO1 calculations do predict a smaller deposition directly in the fuel and a relatively larger deposition in the cladding. This is somewhat advantageous during a LOCA but the effect is small. Of greater interest is the sum of all gamma energy deposited outside of the fuel and cladding. KRISO1 predicts a slightly higher amount than before, 8.94%, as compared with 7.86%.

Also in Table 4-2 is a breakdown of the total energy deposition which includes not only the gamma energy but also the beta energy and fission fragment kinetic energy (in the normal power case). Not included here is the neutron kinetic energy. This will be considered separately.

The total energy deposition is calculated in a straightforward manner based on the gamma energy deposition results and a knowledge of the fractional amount of energy,  $\gamma$ , which is released in the form of gammas.  $\gamma$  for normal and LOCA conditions was calculated in Section 2 and is shown in Table 2-17. The fractional energy deposition in the fuel is equal to  $(1 - \gamma)$ , the fraction of the energy which is *not* in the form of gammas and therefore is assumed to be deposited directly there, plus  $\gamma$  times the fractional gamma energy deposition in the fuel. For all other regions, the total energy deposition is simply equal to  $\gamma$  times the fractional gamma energy deposition in that region. These fractions, expressed as percentages, are given at the bottom of Table 4-2.

Table 4-3 is a similar breakdown for BF1T2. Since this fuel is a 7x7 design with a larger rod diameter than for the 8x8 fuel, there is a slightly higher fractional gamma energy deposition in the fuel due to the slightly higher self-absorption probability. Otherwise the results are similar to the results for 8D250.

The calculation of the amount of neutron energy which is deposited outside of the fuel during normal power operation has been computed by Neuhold and Upham<sup>4</sup>. Since the effect is small and is not present under LOCA conditions, their calculations have not been redone. Their results, which differ slightly for 7x7's, 8x8's, and different channel sizes, are shown in Table 4-4. These calculations were for uncontrolled bundles at 40% voids and an exposure of 10 GWd/t. The total energy deposition in the coolant is simply the sum of these figures plus the appropriate values from Table 4-2 and 4-3 for normal power conditions. No correction is made to the LOCA values.

#### 4.1.2 Rod-to-Rod Gamma Energy Transport

The gamma transport calculations described in the previous subsection are also useful for evaluating the flattening effect which gamma transport has on the rod-by-rod power distribution. Figure 4-1 is an illustration of the rod-by-rod redistribution of energy for 8D250 under LOCA conditions. The top value in each box, which represents a fuel rod, is the relative fission density for that rod. This distribution represents the source or origin of the energy and is normalized to the average of the power-producing rods (a total of 63 in this case). Beneath the fission density is the gamma source distribution. Under LOCA conditions the gamma source is made up entirely of delayed gammas from fission products and is therefore very close to the fission density distribution. The value at the bottom of each box in Figure 4-1 is the relative gamma energy deposition from the KRISO1 calculations. The energy deposition for each rod is the sum of the energy deposited in the fuel and cladding regions but does not include energy deposited in the coolant immediately surrounding each rod.

**Table 4-1  
DESCRIPTION OF BUNDLES USED IN  
GAMMA TRANSPORT CALCULATIONS**

	Bundle	
	8D250	BF1T2
Exposure	0	0
Voids, %	40	40
Lattice	8 x 8	7 x 7
Rod outside diameter, in.	0.493	0.563
Cladding thicknesses, in.	0.034	0.037
Channel thicknesses, in.	0.080	0.080
H <sub>2</sub> O Rods	1	0
Gd Rods	4 at 1.5%	1 at 4%, 3 at 3%

**Table 4-2  
GAMMA ENERGY DEPOSITION FOR 8D250**

	Normal Power		LOCA	
	Scatena & Upham 8 x 8 Reload [0.034 in. cladding, 0.08 in. channel] (%)	KRIS01 [80 batches] (%)	Scatena & Upham 8 x 8 Reload [0.034 in. cladding, 0.08 in. channel] (%)	KRIS01 [80 batches] (%)
Fuel	80.78	78.70 ± 0.39	82.27	80.53 ± 0.34
Cladding	9.56	10.49 ± 0.11	9.87	10.53 ± 0.10
In-Channel Coolant	3.14	3.46 ± 0.06	0.0	0.01 ± 0.001
Channel	4.77	4.99 ± 0.10	4.92	5.28 ± 0.07
Out-Channel Coolant	1.75	2.36 ± 0.06	0.0	0.00
Control Blade	0.0	0.0	2.94	3.65 ± 0.07
Total	100	100	100	100

**Total (Gamma + Beta - Kinetic) Energy Deposition**

	Scatena & Upham ( $\gamma = 0.111$ )	KRIS01 ( $\gamma = 0.105$ )	Scatena & Upham ( $\gamma = 0.47$ )	KRIS01 ( $\gamma = 0.493$ )
Fuel	97.87	97.77	91.67	90.41
Cladding	1.06	1.10	4.64	5.19
In-Channel Coolant	0.35	0.36	0.0	0.0
Channel	0.53	0.52	2.31	2.60
Out-Channel Coolant	0.19	0.25	0.0	0.0
Control Blade	0.0	0.0	1.38	1.80
Total:	100	100	100	100

Table 4-3  
**GAMMA ENERGY DEPOSITION FOR BF1T2**

	Normal Power		LOCA	
	Scatena & Upham 7 x 7 [0.032 in. cladding] (%)	KRIS01 [80 batches 0.037 in. cladding] (%)	Scatena & Upham 7 x 7 [0.032 in. cladding] (%)	KRIS01 [80 batches 0.037 cladding] (%)
Fuel	82.50	79.82±0.37	84.25	31.63±0.35
Cladding	7.58	9.66±0.11	7.78	9.84±0.11
In-Channel Coolant	3.08	3.48±0.05	0.0	0.01±0.001
Channel	4.67	4.79±0.09	4.79	5.11±0.09
Out-Channel Coolant	2.17	2.25±0.06	0.0	0.00
Control Blade	0.0	0.0	3.18	3.41±0.06
Total	100	100	100	100

**Total (Gamma - Beta - Kinetic) Energy Deposition**

	Scatena & Upham ( $\gamma = 0.111$ )	KRIS01 ( $\gamma = 0.105$ )	Scatena & Upham ( $\gamma = 0.47$ )	KRIS01 ( $\gamma = 0.493$ )
Fuel	98.06	97.88	92.60	30.95
Cladding	0.84	1.01	3.66	4.85
In-Channel Coolant	0.34	0.37	0.0	0.0
Channel	0.52	0.50	2.25	2.52
Out-Channel Coolant	0.24	0.24	0.0	0.0
Control Blade	0.0	0.0	1.49	1.68
Total	100	100	100	100

Table 4-4  
**NEUTRON ENERGY DEPOSITION IN COOLANT**  
 (Expressed as a Percentage of Total  
 Energy Deposition)

Fuel Type	Percent Deposition
7 x 7	2.67
8 x 8 (80-mil channel)	2.67
8 x 8 (120-mil channel)	2.39

W-W

1.165 <sup>a</sup>	1.217	1.218	1.143	1.119	1.130	1.185	1.196
1.163	1.213	1.215	1.141	1.117	1.128	1.182	1.193
0.968	1.012	1.077	0.980	1.023	1.045	1.043	1.049
	1.076	1.158	1.091	1.079	1.079	1.127	1.068
	1.075	1.156	1.090	1.078	1.078	1.125	1.066
	1.007	1.063	1.018	1.067	1.058	1.066	1.022
		0.423	0.891	0.909	0.881	0.410	1.147
		0.430	0.893	0.911	0.883	0.417	1.145
		0.841	0.975	0.983	0.989	0.869	1.054
			0.861	0.878	0.856	0.876	1.075
			0.863	0.880	0.857	0.878	1.074
			0.955	1.015	0.951	0.979	0.994
				0.000	0.872	0.893	1.061
				0.000	0.874	0.895	1.060
				0.094	0.939	0.940	1.043
					0.845	0.866	1.062
					0.848	0.868	1.061
					0.944	0.933	0.982
						0.396	1.111
						0.404	1.109
						0.886	1.021
							1.043
							1.041
							0.934

<sup>a</sup>	X.XXX	FISSION DENSITY
	X.XXX	GAMMA SOURCE
	X.XXX	KRISO1 GAMMA ENERGY DEPOSITION (E. 0.034)

Figure 4-1. Rod-by-Rod Gamma Energy Deposition for 8D250 under LCCA Conditions

It will be recalled that the KRIS01 calculations involved 80 batches of 1000 source photons each. This resulted in a standard error of approximately  $\pm 0.034$  for an individual rod energy deposition. This is a rather large statistical error when viewing the results for any single rod. However, what is of interest is not the results for any single rod, but rather the development of a simple model which can account for the overall flattening effect of the gamma transport. Effectively, there are 64 samples available, each with a standard error of 0.034 and therefore the statistical error in the simplified model will be small. In any case, the Monte Carlo calculations are so expensive that extending them further is not economically justified.

It is noteworthy that while the relative gamma source in the gadolinia rods is only about 0.4, the relative energy deposition is about 0.9. This is clear evidence of the mobility of the gamma rays and of the transport of gamma energy between rods.

Figure 4-2 shows the rod-by-rod gamma energy deposition for BF1T2 under LOCA conditions. The results are similar to those for 8D250. The standard error is approximately 0.029 which is lower than before because of the fewer number of rods in BF1T2.

Figures 4-3 and 4-4 show the rod-by-rod gamma energy deposition at normal power conditions for 8D250 and BF1T2, respectively. For these problems, the gamma source differs substantially from the fission density. This is primarily the result of two effects which are related to the capture gamma contribution to the gamma source. The first effect is the spatial distribution of resonance captures in  $U^{238}$ . The second effect is the localization of all of the capture gamma's from gadolinium in a small number of rods. In fact, the locations of the gadolinia rods are clearly evident in Figures 4-3 and 4-4 since their gamma sources are ordinarily double the sources of surrounding rods. The standard error for a typical rod for 8D250 was 0.039 while the standard error for BF1T2 was 0.033.

The Monte Carlo calculations are obviously too expensive to perform routinely and therefore a simple model is necessary which relates the rod-by-rod fission density (which is routinely calculated) and the gamma energy deposition. Let  $f_i$  be the relative fission density of rod  $i$  and let  $P_{\gamma i}$  be the relative gamma energy deposition. These two quantities are related approximately by the following formula:

$$P_{\gamma i} \cong \beta' f_i - (1 - \beta') \tag{4-1}$$

where  $\beta'$  is a fit coefficient which is determined by the least squares method. The simplified model was first developed and utilized by Scatena and Upham<sup>5</sup>.  $\beta'$  is roughly equal to the self-absorption probability of a gamma ray in the rod of its origin. Therefore, different values are required for 7x7 and 8x8 lattices and furthermore different values are required for normal and LOCA conditions. The total rod power or energy deposition,  $p_i$ , is the sum of a direct contribution from fission (kinetic energy of the fission fragments, beta rays, etc.) and a contribution from gamma energy deposition:

$$p_i \cong (1-\gamma)f_i + \gamma(1-S) \left[ \beta' f_i + (1-\beta') \right] \tag{4-2}$$

where  $\gamma$  is the fraction of energy which is in the form of gamma rays and  $S$  is the structural absorption probability for gamma energy. This expression is not normalized in the conventional way since the fraction  $S$  of the gamma energy has been removed. Renormalizing so that the sum of the powers in all of the rods is equal to the number of rods, produces the following result:

$$\bar{p}_i \cong (1-\gamma')f_i - \gamma' \left[ \beta' f_i - (1-\beta') \right] \tag{4-3}$$

when  $\gamma'$  may be thought of as an effective value of  $\gamma$ :

$$\gamma' = \gamma \frac{(1-S)}{1-\gamma S} \tag{4-4}$$

W-W

1.076 <sup>a</sup>	1.063	0.985	1.091	1.107	1.170	1.193
1.073	1.061	0.984	1.089	1.105	1.167	1.190
0.917	0.936	0.958	1.024	1.013	1.046	1.042
	0.273	1.094	1.113	1.122	1.188	1.041
	0.282	1.093	1.112	1.121	1.185	1.040
	0.766	1.035	1.036	1.040	1.069	1.033
		0.928	0.874	0.863	0.359	1.219
		0.929	0.876	0.866	0.368	1.216
		1.008	0.978	1.004	0.827	1.070
			0.324	0.310	0.915	1.177
			0.333	0.313	0.917	1.175
			0.761	0.910	0.966	1.084
				0.376	1.006	1.245
				0.379	1.007	1.242
				1.004	1.056	1.084
					1.131	0.982
					1.130	0.982
					1.040	1.028
						1.159
						1.157
						1.024

<sup>a</sup>	X.XXX	FISSION DENSITY
	X.XXX	GAMMA SOURCE
	X.XXX	KRIS01 GAMMA ENERGY DEPOSITION ( $\pm$ 0.029)

Figure 4-2. Rod-by-Rod Gamma Energy Deposition for BF1T2 under LOCA Conditions

W-W

1.165 <sup>a</sup>	1.217	1.218	1.143	1.119	1.130	1.185	1.196
1.104	1.121	1.112	1.049	1.030	1.039	1.086	1.109
1.005	1.041	1.040	1.039	0.987	1.010	1.028	1.043
	1.076	1.158	1.091	1.079	1.079	1.127	1.063
	0.985	1.040	0.984	0.974	0.975	1.014	0.986
	1.070	1.117	1.020	1.010	1.014	1.013	0.983
		0.423	0.891	0.909	0.881	0.410	1.147
		1.785	0.818	0.833	0.811	1.702	1.038
		1.215	0.928	0.900	0.944	1.251	1.011
			0.861	0.878	0.856	0.876	1.075
			0.795	0.812	0.791	0.807	0.973
			0.958	0.950	0.909	0.964	0.984
				0.000	0.872	0.893	1.061
				0.006	0.806	0.821	0.967
				0.147	0.923	0.918	0.963
					0.845	0.866	1.062
					0.783	0.799	0.963
					0.890	0.910	0.963
						0.396	1.111
						1.612	1.009
						1.109	0.964
							1.043
							0.972
							0.937

<sup>a</sup>	X.XXX	FISSION DENSITY
	X.XXX	GAMMA SOURCE
	X.XXX	KRISO1 GAMMA ENERGY DEPOSITION (± 0.039)

Figure 4-3. Rod-by-Rod Gamma Energy Deposition for 8D250 under Normal Power Conditions

W-W

1.076 <sup>a</sup>	1.063	0.985	1.091	1.107	1.170	1.193
0.991	0.958	0.893	0.972	0.986	1.038	1.071
0.940	1.008	0.954	0.960	1.009	0.988	0.987
	0.273	1.094	1.113	1.122	1.188	1.041
	2.186	0.949	0.964	0.972	1.024	0.932
	1.458	0.988	0.994	0.983	1.026	0.953
		0.928	0.874	0.863	0.359	1.219
		0.818	0.775	0.767	1.663	1.055
		0.952	0.958	0.973	1.278	1.002
			0.324	0.810	0.915	1.177
			1.371	0.725	0.809	1.023
			1.143	0.969	0.955	0.983
				0.876	1.006	1.245
				0.778	0.881	1.076
				0.906	0.955	0.983
					1.131	0.982
					0.981	0.886
					0.992	0.903
						1.159
						1.035
						0.992

<sup>a</sup>	X.XXX	FISSION DENSITY
	X.XXX	GAMMA SOURCE
	X.XXX	KRIS01 GAMMA ENERGY DEPOSITION (≅ 0.033)

Figure 4-4. Rod-by-Rod Gamma Energy Deposition for BF1T2 under Normal Power Conditions

Equation 4-3 may be further simplified by defining the constant A as follows:

$$A \equiv 1 - \gamma(1-\beta') \quad (4-5)$$

Then it can be shown that

$$\bar{p}_i = A f_i + (1-A) \quad (4-6)$$

This is a very simple and convenient-to-use expression.

Table 4-4 is a summary of the numerical constants used in Equations 4-1 through 4-6. The current values from Scatena and Upham<sup>5</sup> are given (where known) along with the new recommended values based on the Monte Carlo calculations. Note that the values of  $\beta'$  for 8D250 and BF1T2 are very close for LOCA conditions while they differ substantially for normal power conditions. Since the new values of A for the 7x7 and 8x8 cases are very close, it was decided to average the two values to obtain a single result. This is consistent with the model currently in use<sup>5</sup> and is a good approximation.

#### 4.1.3 Bundle-to-Bundle Gamma Energy Transport

The calculations in the previous subsection assume that the periphery of the fuel bundle is a mirror or reflecting boundary to gamma rays. In fact, however, the peak power bundle in an operating reactor is surrounded by bundles of lesser power and, therefore, a certain amount of the gamma energy generated in the peak power bundle leaks out to neighboring bundles. This effect was originally quantified by Scatena and Upham<sup>5</sup>. Their results have not been reevaluated for two reasons. The first is that the close agreement between their results and KRISO1 results in the single bundle case is a strong indication that the multi-bundle results would also agree closely. The second reason is that KRISO1 multi-bundle calculations would be extremely expensive and the small improvement in accuracy is therefore not justified.

The approximate physical model for bundle-to-bundle gamma energy transport is very similar to the rod-to-rod model. Let  $F_j$  be the relative fission density of bundle j with respect to neighboring bundles.  $P_{\gamma j}$ , the relative gamma energy deposition, is related approximately to  $F_j$  by the following:

$$P_{\gamma j} \equiv \alpha' F_j - (1 - \alpha') \quad (4-7)$$

where  $\alpha'$  is a parameter which may be thought of as the bundle self-absorption probability.  $\alpha'$  is determined by fitting the results of several calculations. The total bundle power or energy deposition,  $P_i$ , is the sum of a direct contribution from fission (kinetic energy of the fission fragments, beta rays, etc.) and a contribution from gamma energy deposition:

$$\begin{aligned} P_i &\equiv (1 - \gamma) F_i + \gamma P_{\gamma i} \\ &\equiv (1 - \gamma) F_i + \gamma [\alpha' F_i + (1 - \alpha')] \end{aligned} \quad (4-8)$$

where  $\gamma$  is the fraction of energy released in the form of gammas. It is convenient to define a constant C such that:

$$C \equiv 1 - \gamma(1-\alpha') \quad (4-9)$$

Then Equation 4-8 may be simplified:

$$P_i \equiv C F_i - 1 - C \quad (4-10)$$

Table 4-6 shows the values of  $\alpha'$  and C which were obtained by Scatena and Upham<sup>5</sup>. It is recommended that these values be used.

**Table 4-5  
CONSTANTS FOR THE ROD POWER MODEL**

	Normal	LOCA
$\gamma$		
Current (Scatena and Upham)	0.111	0.47
New	0.105	0.493
<b>S</b>		
Current 8 x 8	0.0966	0.0786
New, 8D250	0.1081	0.0894
Current 7 x 7	0.0992	0.0797
New, BF1T2	0.1052	0.0853
$\gamma'$		
New, 8D250	0.0947	0.4696
New, BF1T2	0.0950	0.4707
$\beta'$		
New, 8D250	0.377	0.265
New, BF1T2	0.146	0.285
<b>A</b>		
Current All	0.926	0.685
New 8D250	0.941	0.655
New BF1T2	0.919	0.663
New Combined	0.930	0.659

**Table 4-6  
CONSTANTS FOR THE BUNDLE-TO-BUNDLE MODEL<sup>2</sup>**

	Normal Power	LOCA
$\alpha'$	0.489	0.489
C	0.943	0.760

<sup>2</sup>Obtained from Scatena and Upham<sup>5</sup>.

## 4.2 SPECIFICATIONS FOR ENERGY TRANSPORT MODELS

The gamma and neutron energy transport models described in Subsection 4.1 are applicable to ECCS calculations in two areas. The first area is the calculation of the peak cladding temperature (PCT) and the maximum local oxidation of the cladding. This results in the determination of an operating limit on the maximum average planar linear heat generation rate (MAPLHGR). These calculations are performed in the engineering computer program CHASTE<sup>1</sup>. The second area in which gamma transport is involved is in the determination of whether or not an operating reactor is within the MAPLHGR constraint. This calculation is performed within the process computer. Specifications for the implementation of the gamma transport effect into CHASTE are presented in the text below. This is followed by a discussion of the applicable process computer models.

In general terms, the calculations in CHASTE proceed as follows: First, the bundle power is adjusted so that the peak rod is maintained at the peak linear heat generation rate (PLHGR) of the technical specifications. Then the transient thermo-dynamic and radiation transport calculations are performed to determine the resulting peak cladding temperature and maximum local oxidation. If these quantities are within limits, then the MAPLHGR is simply determined by the average linear heat generation rate as it was first determined. On the other hand, if the limits are exceeded, an iterative process is instituted which adjusts the average linear heat generation rate downwards until the limits are met. It should be remarked that the CHASTE calculations are two-dimensional in nature in that they consider only a horizontal slice through the fuel bundle. Ordinarily, this slice is taken at the peak axial power, but it may also be taken at other locations such as the location of lowest penetration of transition boiling.

More specifically, the CHASTE calculations are as follows. First, the peak rod\* is located by finding the rod with the maximum fission density:

$$f_j^{\max} \geq f_i \quad \text{all } j \quad (4-11)$$

where  $f$  is the relative fission density as determined in the course of the nuclear design. The peak relative power is evaluated using the simplified energy deposition model, Equation 4-6:

$$\bar{P}_j^{\max} = A(0) \cdot f_j^{\max} \cdot \left[ 1 - A(0) \right] \quad (4-12)$$

where  $A$ , the transport fit coefficient, is now understood to be time dependent but is evaluated at normal power or  $t=0$  for the sake of determining the peak rod prior to a LOCA. The average linear heat generation rate in kW/ft,  $A_{LHGR}$ , over the rods in the horizontal slice is now readily determined from the peak linear heat generation rate in kW/ft,  $P_{LHGR}$ :

$$A_{LHGR} = \frac{P_{LHGR} \cdot P_{MLT}}{\bar{P}_j^{\max}} \quad (4-13)$$

where  $P_{MLT}$  is the required multiple of 1.02 which accounts for instrument error.

The bundle power in MW,  $P_{BUNDLE}$ , as it is evaluated in CHASTE, is basically a conversion of  $A_{LHGR}$  to a total bundle basis under the assumption that the axial power shape is uniform. Further corrections are applied to correct for effects taken into account in the process computer (thus avoiding duplication):

$$P_{BUNDLE} = \frac{A_{LHGR} \cdot N_F \cdot C_{LONG} / 12}{1000 \cdot (1 - FCHFLK) \left( B_{PC} - \frac{1 - B_{PC}}{f_{max}} \right)} \quad (4-14)$$

<sup>1</sup>In CHASTE, rods are lumped together into groups. However, this distinction is not important here since the formulas in the gamma transport models apply equally well to groups of rods as well as to individual rods.

where  $N_F$  is the number of fuel (power-producing) rods and  $C_{LONG}$  is the active length of the fuel in inches.  $F_{CHFLK}$  and  $B_{PC}$  are process computer constants which account for structural absorption of gammas and bundle-to-bundle gammas transport, respectively.  $f_{rax}$  is the relative bundle fission density with respect to neighboring bundles.

The time-dependent power in the bundle,  $P(t)$ , is found by multiplying  $P_{BUNDLE}$ , which is essentially the initial power being generated in the bundle, times the relative decay power as a function of time,  $R(t)$ , and, in addition, by multiplying by a correction term which accounts for gamma leakage from the bundle as a function of time:

$$P(t) = P_{BUNDLE} \cdot R(t) \cdot \left( B(t) + \frac{1-B(t)}{f_{rax}} \right) \quad (4-15)$$

where  $B(t)$  is the time-dependent bundle-to-bundle transport coefficient. It must be pointed out that ordinarily  $f_{rax}$  is not known at the time of CHASTE calculations are being performed. The inclusion of the bundle-to-bundle factors in Equations 4-14 and 4-15 is useful only for parametric studies. If such studies are not required then it is a simple matter to set  $B_{PC}=B(t)=1$ .

The gamma energy sharing between fuel rods is a function of time as was pointed out previously. Generalizing Equation 4-6 to the time-dependent case results in the following:

$$\bar{P}_i(t) = A(t) \cdot f_j - [1-A(t)] \quad (4-16)$$

The distribution of the total power  $P(t)$  among the various structural components of the bundle is governed by the fractional energy deposition rates discussed in Subsection 4.1.1. These fractions must now be considered to be time-dependent quantities. Let  $F_x(t)$  be the fractional energy deposition in region  $x$  where  $x=f$  stands for the fuel rods,  $C$  stands for the cladding,  $W$  for water rods,  $CH$  for the channel,  $BL$  for the blade and  $CO$  for the coolant. The power generated in a given fuel rod may now be expressed as follows:

$$P_{fi}(t) = P(t) \cdot F_f(t) \cdot \bar{P}_i(t)/N_f \quad (4-17)$$

where division by the total number of power-producing fuel rods  $N_f$  is required since the distributions  $\bar{P}_i(t)$  and  $f_j$  are normalized such that the sum over all  $j$  is equal to  $N_f$ . The power generated in the cladding of rod  $j$  is:

$$P_{ci}(t) = P(t) \cdot F_c(t) \cdot \bar{P}_i(t)/N_f \quad (4-18)$$

If a water rod is located at position  $j$  then:

$$\begin{aligned} P_{fi}(t) &= 0.0 \\ P_{ci}(t) &= P(t) \cdot F_w(t)/N_w \end{aligned} \quad (4-19)$$

The power generation rates in the channel, blade, and coolant are readily determined as follows:

$$\begin{aligned} P_{CH}(t) &= P(t) \cdot F_{CH}(t) \\ P_{BL}(t) &= P(t) \cdot F_{BL}(t) \\ P_{CO}(t) &= P(t) \cdot F_{CO}(t) \end{aligned} \quad (4-20)$$

It should be noted in passing that the sum of all fractional energy depositions is unity:

$$F_f(t) + F_c(t) - F_w(t) + F_{CH}(t) + F_{BL}(t) + F_{CO}(t) = 1 \quad (4-21)$$

\*The current decay heat model is equivalent to  $R(t)=R_i(t)$ . The recommended model  $R_i(t,E)$  has an additional argument, the fuel exposure. The proposed model  $R_{ii}(t,T,E)$ , which may be used only for evaluation purposes, has as a third argument, the irradiation time. For the purpose of the current discussion, all three models are interchangeable.

Therefore, the sum of the powers in all regions is equal to the total power:

$$\sum_j \left( P_{fj}(t) + P_{c_j}(t) \right) \cdot N_j - P_{CH}(t) - P_{BL}(t) - P_{CO}(t) = P(t) \tag{4-22}$$

where  $N_j$  is the number of rods in group  $j$ . This is the expected result.

The time dependence of the fractions  $F_x(t)$  must be approximated in some way. In Subsection 4.1.1 two steady-state calculations were performed: one at normal power conditions and the other at LOCA conditions. At time zero,  $F_x(t)$  will have the value corresponding to normal power conditions. At long times after the initiation of the LOCA, the value of  $F_x(t)$  will correspond to the LOCA value. At intermediate times, while the fission power is decaying, the value will be in between the normal and LOCA values. It is theoretically possible to use the decay heat curves along with the fission power curves to compute the exact value, but the complexity of such a method is not warranted. The simplified method, which is currently in use and which has been shown to be conservative<sup>5</sup>, is to assume that  $F_x(t)$  varies linearly with time up until the time,  $t_L$ , when the fission power decays to less than 1% of its original value. Thereafter,  $F_x(t)$  takes on a constant value equal to the value for LOCA conditions. From Table 3-5, the value of  $t_L$  may be taken to be equal to 6 seconds. The time dependence of the fractions  $F_x(t)$  is explicitly shown in Table 4-7. In addition,  $A(t)$ , the parameter in Equation 4-16, and  $B(t)$ , the parameter in Equation 4-15, are also assumed to have a similar dependence as shown in this table. The fraction  $F_f(t)$  is evaluated by rearranging Equation 4-21:

$$F_f(t) = 1 - F_C(t) - F_W(t) - F_{CH}(t) - F_{BL}(t) - F_{CO}(t) \tag{4-23}$$

**Table 4-7**  
**TIME DEPENDENCE OF THE PARAMETERS**

Parameters	t = 0	0 < t < t <sub>L</sub>	t > t <sub>L</sub>
F <sub>C</sub> (t)	FCZ	FCZ - t/t <sub>L</sub> (FCL-FCZ)	FCL
F <sub>W</sub> (t)	FWZ	FWZ - t/t <sub>L</sub> (FWL-FWZ)	FWL
F <sub>CH</sub> (t)	FCHZ	FCHZ - t/t <sub>L</sub> (FCHL-FCHZ)	FCHL
F <sub>BL</sub> (t)	FBLZ	FBLZ - t/t <sub>L</sub> (FBLL-FBLZ)	FBLL
F <sub>CO</sub> (t)	FCOZ	FCOZ - t/t <sub>L</sub> (FCOL-FCOZ)	FCOL
A(t)	AZ	AZ - t/t <sub>L</sub> (AL-AZ)	AL
B(t)	BZ	BZ - t/t <sub>L</sub> (BL-BZ)	BL

Values for the constants in Table 4-7 are given in Table 4-8. The name of the constant is given in the first column and its value is column two. The third column describes the fuel type for which it is applicable. The fourth column states the method used to calculate the value. The values labeled KRIS01 are the result of the calculations described in Subsection 4.1.1 and 4.1.2. All other values have been obtained by an approximate method. This method is based on correcting the KRIS01 results for changes in the amount of material present. For example, the value of FCZ, the fraction of energy deposited in the cladding at normal power, for a 7x7 lattice with 32-mil cladding is found by multiplying the KRIS01 value for a 7x7 lattice with 37-mil cladding by the ratio of the volume of the 32-mil cladding to the volume of the 37-mil cladding. Since both claddings have the same diameter, this volume ratio is very close to the ratio of the cladding thicknesses. All other constants are evaluated in similar ways.

After the completion of the CHASTE calculations and assuming that the peak cladding temperature and maximum local oxidation are within limits, the MAPLHGR may be computed as follows:

$$M_{APLHGR} = A_{LHGR}/1.02 \tag{4-24}$$

The division by 1.02 removes the multiple which accounts for instrument error so that the MAPLHGR may be compared directly with instrument readings at the plant site.

Table 4-8  
VALUES FOR GAMMA TRANSPORT COEFFICIENTS

Name	Value	Fuel	Method
AZ	0.930	All	KRIS01
AL	0.659	All	KRIS01
FCZ	0.0087	7 × 7 (32-mil cladding)	0.0101 × 32/37
	0.0101	7 × 7 (37-mil cladding)	KRIS01
	0.0102	8 × 8 (32-mil cladding, 1 H <sub>2</sub> O rod)	0.0108 × 32/34
	0.0100	8 × 8 (32-mil cladding, 2 H <sub>2</sub> O rod)	0.0102-0.0002
	0.0108	8 × 8 (34-mil cladding, 1 H <sub>2</sub> O rod)	KRIS01
	0.0106	8 × 8 (34-mil cladding, 2 H <sub>2</sub> O rod)	0.0108-0.0002
FCL	0.0419	7 × 7 (32-mil cladding)	0.0485 × 32/37
	0.0485	7 × 7 (37-mil cladding)	KRIS01
	0.0482	8 × 8 (32-mil cladding, 1 H <sub>2</sub> O rod)	0.0512 × 32/34
	0.0475	8 × 8 (32-mil cladding, 2 H <sub>2</sub> O rod)	.0482-0.0007
	0.0512	8 × 8 (34-mil cladding, 1 H <sub>2</sub> O rod)	KRIS01
	0.0505	8 × 8 (34-mil cladding, 2 H <sub>2</sub> O rod)	0.0512-0.0007
FWZ	0.0002	8 × 8 (1 H <sub>2</sub> O rod)	KRIS01
	0.0004	8 × 8 (2 H <sub>2</sub> O rod)	0.0002 · 2
FWL	0.0007	8 × 8 (1 H <sub>2</sub> O rod)	KRIS01
	0.0014	8 × 8 (2 H <sub>2</sub> O rod)	0.0007 · 2
FCHZ	0.0050	7 × 7 (80-mil char.net)	KRIS01
	0.0052	8 × 8 (80-mil channel)	KRIS01
	0.0065	8 × 8 (100-mil channel)	0.0052 × 100/80
	0.0078	8 × 8 (120-mil channel)	0.0052 × 120/80
	0.0252	7 × 7 (80-mil channel)	KRIS01
FCHL	0.0260	8 × 8 (80-mil channel)	KRIS01
	0.0325	8 × 8 (100-mil channel)	0.0260 × 100/80
	0.0390	8 × 8 (120-mil channel)	0.0260 × 120/80
	0.0	All	KRIS01
FBLZ	0.0168	7 × 7	KRIS01
FBLL	0.0180	8 × 8	KRIS01
	0.0180	7 × 7	KRIS01
FCOZ	0.0328	7 × 7	0.0061 (KRIS01) - 0.0267
	0.0328	8 × 8 (80-mil channel)	0.0061 (KRIS01) - 0.0267
	0.0314	8 × 8 (100-mil channel)	0.0061 (KRIS01) - (0.0267 - 0.0239) · 2
	0.0300	8 × 8 (120-mil channel)	0.0061 (KRIS01) - 0.0239
FCOL	0.0	All	KRIS01

The second major area in which gamma transport effects must be considered is in the process computer. The process computer is related to ECCS calculations through the MAPLHGR, which is used to ascertain that the fuel is operating within limits. In performing its calculations, the process computer makes use of two gamma transport effects: absorption in structural materials and bundle-to-bundle transport.

Within the process computer, each fuel bundle is divided into 6-inch axial segments. The power,  $P_s$ , for each segment is calculated from instrument readings with corrections based on the bundle environment. An average "four-bundle" segment power is then computed for each four-bundle group surrounding an instrument tube (or pseudo tube). Equation 4-10 is then employed to compute the true energy deposition within the segment:

$$\frac{\bar{P}_s}{P_{4B}} = C \frac{P_s}{P_{4B}} + (1-C) \quad (4-25)$$

The segment power is then corrected for structural absorption and converted to kW per foot as follows:

$$APLHGR = \frac{\bar{P}_s \cdot 10^3 \cdot (1 - FLK - FCH)}{N_R \cdot L_z} \quad (4-26)$$

where  $N_R$  is the number of rods,  $L_z$  the axial length of the segment, FLK is the fraction of power generated in the leakage flow path and FCH is the fraction of power generated in the channel. If APLHGR is less than MAPLHGR from Equation 4-24 then the bundle is within limits and the peak cladding temperature would not be exceeded during a LOCA.

Typical values for the constants in the process computer are as follows:

$$\begin{aligned} FCH &= 0.021 \\ FLK &= 0.019 \\ C &= 0.76 \end{aligned} \quad (4-27)$$

FCH and FLK are bundle dependent, but in most cases their sum is 0.04. It is this value which should be used for the constant FCHFLK in Equation 4-14. The value of C which is used is the value for LOCA conditions (see Table 4-6). This is an approximation which assumes that the impact of bundle-to-bundle gamma transport is determined solely by the LOCA value and is insensitive to the true value for the first 6 seconds of the transient. This approximation has been tested and found to be valid.

## 5. NUCLEAR CORE DESIGN DATA

Nuclear core design data enter into ECCS calculations in three major ways. The most significant way is through nuclear lattice design calculations in the form of rod-by-rod fission density, power, and exposure distributions which are utilized in the peak cladding temperature calculations in the computer program CHASTE. A second way is through steady-state axial power shapes which are input to the transient critical power calculations in SCAT<sup>11</sup> and the short-term thermal-hydraulic calculations in LAMB<sup>11</sup>. A third way is through pellet radial power shapes which are used to calculate gap-conductances which, in turn, are fed into the CHASTE and SCAT calculations. Each of these three areas is either covered by a Licensing Topical Report<sup>15,16</sup> or in the case of the third area, is known to be a small effect. Therefore, the review in these areas has been superficial.

The lattice analysis program<sup>13</sup> which is used in nuclear design calculates, among other things, the relative rod-by-rod fission density and the relative rod-by-rod power. The latter distribution is based on an explicit calculation of the fission and capture gamma source in each rod, followed by a correction for gamma transport effects using Equation 4-1. Then the direct contribution from fission, the fragment kinetic energy and the beta energy, is added back to produce the total power. This rod power distribution is then transmitted to an engineering computer program which performs two functions. It computes fuel rod exposures for use in the gap conductance calculations and it produces estimated rod-by-rod fission densities for input to CHASTE. The procedure for estimating the fission densities is based on the inversion of Equation 4-6 to provide an expression for the fission density in terms of the power:

$$f_i = \frac{1}{A} P_i + \left(1 - \frac{1}{A}\right) \quad (5-1)$$

The values of A which are used depend on the number of rods in the lattice and were developed from lattice analysis results through a fitting procedure. These values are shown in Table 5-1 along with the current ECCS value and the new recommended value from Table 4-4. Although the differences are small, it is recommended that the new value be used in design work for all lattices.

Table 5-1  
VALUES FOR GAMMA TRANSPORT PARAMETER A

Use	Lattice	A (Normal Power)
Design	7 × 7	0.922
Design	8 × 8	0.925
Design	9 × 9	0.927
Current ECCS	All	0.926
New Recommended	All	0.930

The sensitivity of ECCS calculations to axial power shape has been considered elsewhere<sup>11</sup> and has not been reviewed here.

The radial power shape within fuel pellets is determined from fits based on initial enrichment, pellet diameter, exposure, etc. In evaluating these fits for the purpose of gap conductance calculations, a single enrichment is used which corresponds to the average enrichment of all pellets in the lattice. This is a conservative assumption since the interior rods, which are the hottest during a LOCA, have a higher than average enrichment and hence a radial power which is somewhat more peaked to the outside. This tends to allow for more rapid cooling. In order to estimate the magnitude of the conservatism, several CHASTE calculations at varying exposures were made using a single radial power shape for all pellets based on the average pellet enrichment. The results were then compared with calculations which assumed that the radial power shape was flat for all pellets. The peak cladding temperatures were higher in the latter cases by approximately 10°F for the low exposure cases and by 20°F for the high exposure cases. The varying differential is due to the build up of plutonium near the surface of the pellets. In any case, the effect of considering the precise radial power shape in each pellet is obviously a much smaller effect and can be neglected without being over conservative.

## 6. CONCLUSIONS

As a result of this review, a number of improvements are possible in the nuclear basis for ECCS calculations. New values have been obtained for the energy yields from fission of  $U^{235}$ ,  $U^{238}$ , and  $Pu^{239}$ . New values have also been obtained for the decay energies of the important actinides  $U^{239}$  and  $Np^{239}$ .

In the area of decay heat calculations, a new model has been presented which is more accurate than the current model and removes some of the over conservatism. In particular, a 1% to 2% reduction in decay heat is predicted by this model when compared with the current model, even though both are based upon the current ANS-5 standard. Another decay heat model which is based on the ANS-5.1 subcommittee's proposed standard and which is believed to be even more accurate, shows an even greater reduction in decay heat, on the order of 15% to 20%, when compared with the current model. This proposed model illustrates the large degree of conservatism in the current model.

In the area of nuclear energy transport and deposition, several photon Monte Carlo calculations were used to determine new values for gamma transport parameters. Although the net impact of these new values on ECCS calculations will be very small, the fact that a more accurate method has been used to generate them, along with the fact that the gamma transport models, within which these values are used, have also been reviewed and found to be adequate, serves to increase overall confidence in the ECCS calculations.

A very brief review of the nuclear core design data which is input to ECCS calculations has also resulted in the conclusion that the data is acceptable and consistent with ECCS usage.

## 7. REFERENCES

1. Title 10, Code of Federal Regulations, Part 50, Appendix K—"ECCS Evaluation Models."
2. "Proposed ANS Standard—Decay Energy Release Rates Following Shutdown of Uranium-Fueled Thermal Reactors," American Nuclear Society, draft, Oct. 1971.
3. "Proposed ANS Standard—Decay Energy Release Rates Following Shutdown of Uranium-Fueled Thermal Reactors," American Nuclear Society, Oct. 1971. Revised Oct. 1973.
4. "Proposed Revised ANS Standard (ANS-5.1) Decay Heat Power in Light Water Reactors for Shutdown Times Less than 10<sup>4</sup> seconds," American Nuclear Society, March 1977.
5. G. J. Scatena, G. L. Upham, *Gamma Heating Distribution in a BWR Lattice During Normal Operation and Accident Conditions*, (NEDE-10792), December 1973.
6. J. P. Unik and J. E. Gindler, *A Critical Review of the Energy Released in Nuclear Fission*, Argonne National Laboratory, March 1971, (ANL-7748).
7. R. Sher, et al., *Fission Energy Release for 16 Fissioning Nuclides*, October 1976, attached as Appendix A to enclosure 9 of S. Pearlstein, *Summary of CSEWG Meeting, October 27-28, 1976*, December 10, 1976.
8. W. H. Walker, *The Use of Averages and Other Summation Quantities in the Testing of Evaluated Fission Product Yield and Decay Data. Applications to ENDFB(IV)*, Atomic Energy of Canada, Ltd., January 1976. (AECL-5259).
9. C. M. Lederer, et al., *Table of Isotopes*, sixth edition, John Wiley & Sons, 1967.
10. J. C. Widman, et al., "Average Energy of Beta Spectra," *Int. J. of Applied Radiation and Isotopes*, 19, 1-14 (1968).f
11. J. Duncan, et al., *General Electric Company Analytical Model for Loss-of-Coolant Analysis in Accordance with 10CFR50 Appendix K*, General Electric Co., Licensing Topical Report, Volumes I and II, November 1975. (NEDO-20566).
12. *Chart of the Nuclides*, Knolls Atomic Power Laboratory, revised, April 1972.
13. C. L. Martin, *Lattice Physics Methods*, General Electric Co., Licensing Topical Report, February 1977. (NEDO-20913A).
14. P. Neuhold and G. L. Upham, *Determination of Lattice Energy Deposition Distribution*, November 1974. (NEDE-21004).
15. C. L. Martin, *Lattice Physics Methods Verification*, General Electric Co., Licensing Topical Report, June 1976. (NEDO-20939).
16. G. R. Parkos, *BWR Simulator Methods Verification*, General Electric Co., Licensing Topical Report, May 1976. (NEDO-20946).

**DISTRIBUTION**

Name	M/C
S. C. Bhatt .....	151
L. S. Bohl .....	166
R. L. Crowther .....	151
E. C. Hansen .....	190
C. L. Hilf .....	682
R. T. Hill .....	682
C. M. Kang .....	151
A. J. Levine .....	682
C. L. Martin (2) .....	190
A. S. Rao .....	194
W. S. Rowe .....	765
B. S. Shiralkar .....	186
J. M. Sorensen .....	195
R. N. Woldstad .....	682
J. E. Wood .....	148
NEBG Library (5) .....	328
VNC Library (2) .....	V01
Technical Information Exchange (5) .....	SCH
Technical Support Services (2) .....	461
University Libraries (2) .....	



TECHNICAL INFORMATION EXCHANGE

TITLE PAGE

AUTHOR	SUBJECT	TIE NUMBER
C. L. Martin	Nuclear Science & Technology	77NED306
TITLE		DATE
Nuclear Basis For ECCS (Appendix K) Calculations		November 1977
		GE CLASS
		GOVERNMENT CLASS
REPRODUCIBLE COPY FILED AT TECHNICAL SUPPORT SERVICES, R&UO, SAN JOSE, CALIFORNIA 95125 (Mail Code 211)		NUMBER OF PAGES
<p>SUMMARY</p> <p>A comprehensive review of the nuclear basis for ECCS (Appendix K) calculations is presented. The areas covered include: basic nuclear data, nuclear energy sources, nuclear energy transport, and nuclear core design data. New values are proposed for the energy yield per fission of a number of isotopes including <math>U^{235}</math>, <math>U^{238}</math>, and <math>Pu^{239}</math>. A new, more rigorous decay heat model based on the current American Nuclear Society Standard ANS-5 is developed. In addition, a decay heat model based on the ANS-5.1 subcommittee's new decay heat curves is presented for use in evaluating the impact of the proposed standard. In the area of nuclear energy transport, Monte Carlo calculations have been performed to provide more accurate parameters for gamma energy transport.</p>		

By cutting out this rectangle and folding in half, the above information can be fitted into a standard card file.

DOCUMENT NUMBER NEDO-23729

INFORMATION PREPARED FOR Nuclear Energy Engineering Division

SECTION Nuclear Core Technology

BUILDING AND ROOM NUMBER Bldg. 1900, Rm 526 MAIL CODE 190